Final Technical Report

External Grant Award Numbers: **G23AP00242** and **G23AP00244**

Recipients:
Board of Regents of the Nevada System of Higher Education on Behalf of The University of Nevada, Reno (242)
And
The University of Cincinnati (244)

Principal Investigators and authors:
John N. Louie
Nevada Seismological Laboratory, University of Nevada, Reno, and Terēan
MS 174, UNR, Reno, NV 89557, jlouie@terean.com, phone 775 674 9525, fax 775 784 4165
and
Daniel M. Sturmer
Department of Geosciences, University of Cincinnati
345 Clifton Ct., Cincinnati, OH 45221-0013, sturmedm@ucmail.uc.edu, phone 513 556 5705, fax 513 556 7169

With contributions from:

Paul Smith (Departments of Physics and Geosciences, UC Undergraduate Student);
Odesza Gautschi, Gavin Castle, Evan Frossard, Andrea Oviatt, Madeline Darnall, Jazmin Juarez, Ana Amaya, Jack Rowin, Cade Beadell, Maddy Murphy, Benjamin Doughty, Sara Wilson, Kiana Hillis (UNR-CTEMPs Interns);
Kayleigh Dohm, Rob Fuller (UNR-Geosciences Graduate Students)
Ekaansh Meharwal, Ian Rodgers, Xavier Sweet (UC Geosciences Undergraduate Students)
Vincent Nowaczewski, Nirusha Shrestha (UC Geosciences Graduate Students)
Sara Sayyadi (UNR-CTEMPs Postdoc)
Chris Kratt (UNR-CTEMPs)

Title:
Building a CVM for Seismic Resilience in Western Nevada's Industrial Base: Collaborative Research with the Univ. of Nevada, Reno and Univ. of Cincinnati

Project Term:
May 2023 – August 2024

This material is based upon work supported by the U.S. Geological Survey under Grant Numbers G23AP00242 and G23AP00244. The views and conclusions contained in this document are those of the authors and should not be interpreted as representing the opinions or policies of the U.S. Geological Survey. Mention of trade names or commercial products does not constitute their endorsement by the U.S. Geological Survey.

Abstract

Accurate community velocity models are critical for understanding and modeling potential earthquake shaking hazards. One of the critical priorities for the Intermountain West under Element III is to collect data that allow for improvement in community velocity models, particularly in areas that are of economic importance. In Western Nevada, the logistics and manufacturing industries have expanded rapidly in two valleys on the outskirts of the Reno Metro Area. Stead/Lemmon Valley and the Tahoe Reno Industrial Center (TRIC) in the Virginia Range now provide tens of thousands of jobs, and account for most of the employment growth in Nevada outside of Las Vegas. However, recent work on the Reno-area basin did not evaluate potential earthquake shaking or basin amplification in these valleys. Therefore, in this study we combine gravity, seismic, and well log analysis to elucidate shear-wave velocity structure to 1 km depth and constrain basin floor geometries within Lemmon Valley and TRIC.

In this study the University of Nevada, Reno and the University of Cincinnati, in collaboration with Terēan, collected seven seismic and six gravity profiles total in Lemmon Valley and TRIC. The data from Lemmon Valley show an elongate N-trending basin that deepens southward to ~800 m depth. The basin is narrow and bounded by normal faults on both sides. In contrast, the Quaternary basin in TRIC is shallow, mostly less than 50 m deep. The shallow basin combined with the thick Cenozoic volcanic section made applying the suite of techniques we used in Lemmon Valley difficult to carry over to TRIC.

The newly-resolved basins have been added to the Community Velocity Model (CVM) for the Reno area. This higher-resolution CVM will allow the western Nevada community to have a more thorough and nuanced understanding of the shear-wave velocity structure and site response to shaking within TRIC and Lemmon Valley. The updated CVM will be useful to urban planners, developers, and researchers, which is critical in these economic centers of the Intermountain West.

Introduction

The Reno-Carson City-Fernley urban corridor area is one of the most populated and rapidly growing areas within the intermountain west. As of 2020, the area had a population of over 650,000 people, the majority of whom live in the Reno-Sparks area (US Census Bureau, 2021). The population of Washoe County (where Reno and Sparks are located) has increased 13.5% since 2010 and has more than doubled (up 249%) since 1980. Almost all of the recent growth in the logistics and manufacturing industries in western Nevada has been north of Reno (Lemmon Valley) and along Interstate Highway 80 east of Reno (Tahoe-Reno Industrial Center or TRIC; Figure 1). Manufacturing employment in the Reno area has nearly tripled since 2011 (US Bureau of Labor Statistics, 2022). Much of the growth in population has been pushed into the valleys north of Reno-Sparks proper, following the increased industrial employment in the Stead area in Lemmon Valley, 14 km northwest of central Reno.

Figure 1. Google Earth map showing study locations.

The largest industrial park in the US and the third largest in the world (WorldAtlas.com, 2022), the Tahoe-Reno Industrial Complex or TRIC has been developed in the past decade in a valley within the Virginia Range 28 km east of Reno (Figure 1). As one example of the key role TRIC and Lemmon Valley play in Nevada's economy, the Nevada State Rail Plan (2021) specifically identifies the improvement of freight rail access to both TRIC and Lemmon Valley as two of just nine primary rail freight development opportunities Statewide. The Rail Plan also proposes the development of passenger rail service from Reno to TRIC as Nevada's first-ever commuter rail development. TRIC has very few residents, so over 12,000 workers commuted daily from Reno-Sparks to TRIC in 2021, which the Rail Plan expects to double in coming years. Example key

employers and economic drivers at TRIC are the Apple data center, the Switch data center (promoted as the largest in the world), and the Tesla Gigafactory I, itself with over 8000 employees. Prominent logistics employers in Stead / Lemmon Valley include a JC Penney distribution center and an Amazon fulfillment center.

Experience during Covid-19 suggests that minimal business disruption following a major earthquake is of key economic importance. Eckert et al. (2021) found extreme levels of shaking, and high degrees of shaking variation and uncertainty for a magnitude 6.3 quake in the relatively shallow Reno-area basin. Properly preparing business operations and facilities in the face of such a hazard is important for the economy of Nevada as well as the Nation. This project undertakes the challenge of assessing the hazards of basin amplification of shaking in these key industrial areas just outside Reno.

Recent detailed work has using the refraction microtremor (ReMi) technique (Louie, 2001; Louie et al., 2021) has been used to characterize shear-wave velocities in the Reno area (e.g., Pancha et al., 2015; 2017; Pancha and Pullammanappallil, 2014; Pullammanappallil, 2016; Louie, 2020; Simpson and Louie, 2020). However, none of these assessments included TRIC or the North Valleys. With the growing importance of these industrial areas to Nevada's economy, it is critical to extend the Reno-area community velocity models used by Eckert et al. (2021) for scenario shaking computation to these areas, enabling assessment of basin effects on earthquake ground shaking to these critical facilities. Therefore, in this project we combined new and existing gravity (e.g., Jachens and Moring, 1990; Saltus and Jachens, 1995; Abbott and Louie, 2000; Cashman et al., 2012; Widmer, 2023), ReMi, horizontal-vertical spectral ratio analysis (HVSR) (e.g., SESAME, 2005; Bonnefoy-Claudet et al., 2006; Ullah and Luiz Prado, 2016; Perton et al., 2020), and water well logs to better characterize the subsurface in these areas critical to the infrastructure and economy of the Reno-Sparks metro area.

Background

Lemmon Valley is one of a series of valleys north of Reno that are collectively called the "North Valleys". These include Lemmon Valley, Golden Valley, Stead, Panther Valley, Sun Valley, Hungry Valley, and Cold Springs/White Lake Valley. US-395 cuts across the southern part of the North Valleys, connecting Reno to the south and Susanville, CA to the north. The area sits at the intersection of the western Basin and Range province and the Pyramid Lake domain of the Walker Lane. This part of the Basin and Range is characterized by ~north-striking normal faults that have resulted in formation of alternating north-trending mountain ranges and valleys. The Pyramid Lake domain of the Walker Lane (e.g., Stewart, 1988; Faulds et al., 2005; Wesnousky, 2005a, 2005b; Faulds and Henry, 2008) is dominated by NNW-striking, left-stepping, right-lateral strike slip faults that extend between Fernley, NV and Susanville, CA. Mapping efforts in the 1980's showed several north-striking normal faults that cut across the Lemmon Valley (Soeller and Nielsen, 1980; Cordy and Mansour, 1985). However, there are no detailed studies on these faults (USGS and NBMG, 2015). The Peavine Peak fault zone bounds the south end of the basin. The Peavine Peak fault shows evidence for at least four Holocene earthquakes (Ramelli et al., 2003).

The geology around the North Valleys is dominated by Mesozoic bedrock and Quaternary sediments. The mountains surrounding Lemmon Valley are dominantly Triassic-Jurassic

metamorphosed volcanic rocks of the Peavine sequence, Cretaceous granitic rocks, and local Oligo-Miocene welded ash-flow tuffs (Soeller and Nielsen, 1980; Cordy and Mansour, 1985; Ramelli et al., 2011). Miocene alluvial and fluvio-lacustrine sediments are locally exposed around the edges of the valleys. These are likely equivalent (at least in age) to the sandstone of Hunter Creek in Reno (e.g., Kelly and Secord, 2009; Trexler et al., 2012). The valleys contain a variety of unconsolidated Quaternary deposit types, including alluvial fan, fluvial, lacustrine, playa, and aeolian deposits (Soeller and Nielsen, 1980; Cordy and Mansour, 1985; Ramelli et al., 2011). Much work has been done on the hydrology of the Lemmon Valley area (see a recent summary and synthesis by Hanford, 2024).

The Tahoe-Reno Industrial Center (TRIC) is located along the I-80 and Truckee River corridor between Reno and Fernley, NV. The area sits within the Carson domain of the Walker Lane, which is dominated by ENE-striking left-lateral faults and lineaments (Stewart, 1988; Faulds et al., 2005; Faulds and Henry, 2008; Sturmer and Faulds, 2018). The main fault exposed in the area is the Olinghouse fault, which is an oblique normal left-lateral fault broken into numerous strands in the northern part of the TRIC and north of TRIC (e.g., Cashman and Fontaine, 2000; Briggs et al., 2005; Sturmer, 2007; Li et al., 2017; Sturmer and Faulds, 2018).

Unlike the Lemmon Valley area, lithologies in the TRIC are dominated by Mio-Pliocene volcanic units. The northern boundary of the TRIC along the southern Pah Rah Range contains mafic rocks of the Pyramid sequence (e.g., Rose, 1969; Sturmer and Faulds, 2018). The Pyramid sequence is a >1 km thick sequence of dominantly basaltic flow and flow breccias that originated south of Pyramid Lake in the northern part of the Pah Rah Range (e.g., Sturmer and Faulds, 2018). On the southwestern side of the TRIC is the Clark Mountain volcano, which is dominantly Miocene mafic to intermediate volcanic flows (e.g., Schwartz and Faulds, 2004). The eastern side of the basin is bounded by the northern Virginia Range, which also contains Pyramid sequence rocks, along with a thick diatomite deposit and underlying intermediate-mafic units (Rose, 1969; Faulds et al., 2008). At the eastern end of the Truckee River Canyon near Fernley, Oligo-Miocene ask-flow tuffs fill a fluvial channel that was eroded into Mesozoic metamorphic and igneous basement units (Rose, 1969; Faulds et al., 2008; Sturmer and Faulds, 2018). Quaternary units within the TRIC include alluvial fan deposits, lacustrine deposits from Lake Lahontan, and fluvial deposits surrounding the Truckee River (Rose, 1969; Faulds et al., 2008; Sturmer and Faulds, 2018).

Methods

In order to update the CVM, we evaluated basin depth and velocity structure using a combination of gravity, passive-source seismic, well log analysis, and geologic analysis methods (Figure 2). These each discussed below.

Gravity

Data Collection

Gravity data were collected during summer and fall 2023. The gravity survey collection was led by undergraduates Paul Smith (UC) and Odesza Gautschi (UNR). Data were collected using a

CG-6 gravimeter borrowed from CTEMPs (UNR). Position and elevation were measured with a Trimble R10 GPS unit with an RTX subscription for real-time differential positioning, resulting in 5-10 cm elevation accuracy. Gravity measurements were taken for 30 seconds, with a 10 Hz sample rate and a minimum of two measurements per station. To account for instrument drift and tidal variations not handled onboard by the CG-6, measurements at a calibrated NGS gravity base on the UNR Campus in the Scrugham building preceded and followed each day's measurements. Field base stations were also established for repeat measurements every 2-3 hours.

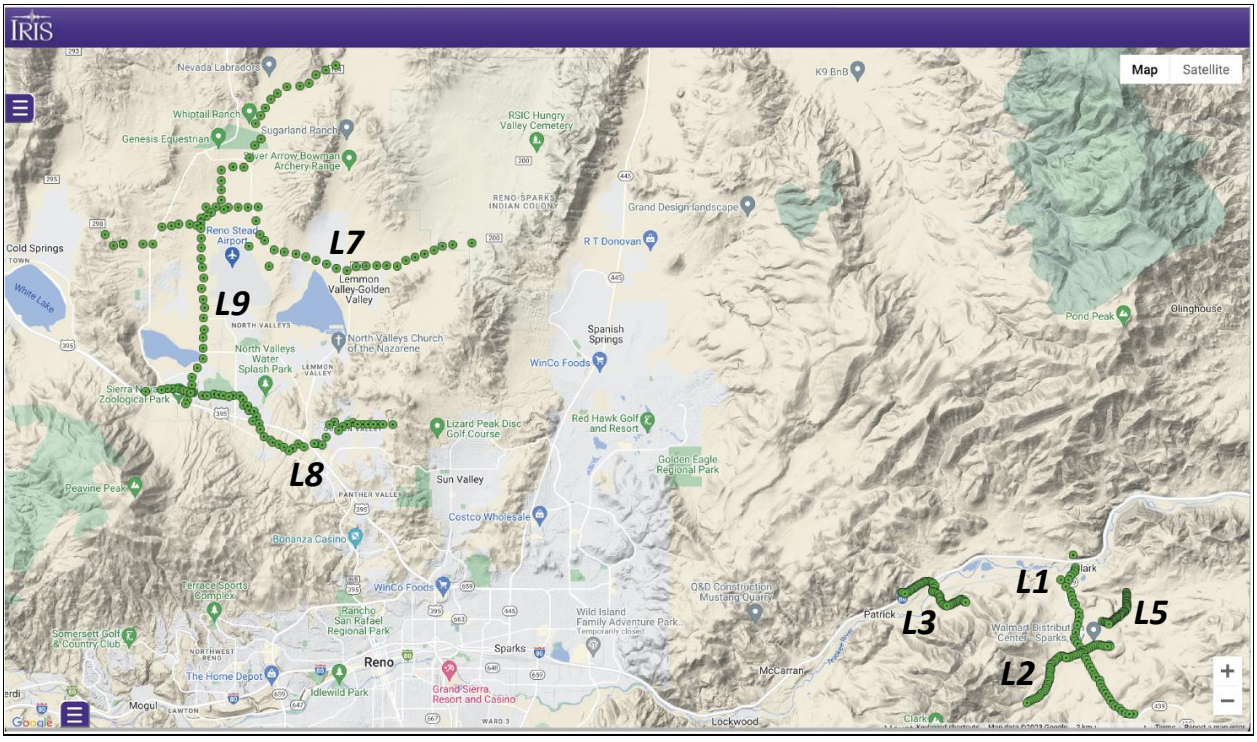

Figure 2. PASSCAL Fairfield 3-component Nodal station locations for this project's deep refraction microtremor and gravity surveys in Lemmon Valley north of Reno and the Tahoe-Reno Industrial Center east of Reno. Station locations given by the IRIS data archive available from http://ds.iris.edu/gmap/#network=5K&planet=earth

Processing

All data reduction, processing, and modeling were done using GM-SYS and Oasis Montaj from Seequent. Gravity loop closures averaged 10 μGal, together with 10 cm elevation uncertainty suggesting a simple Bouguer anomaly uncertainty of 30 μGal. Complete Bouguer anomalies (CBA) including near and far terrain corrections were calculated for the data collected during this study and pre-existing gravity measurements from John Louie (Abbott and Louie, 2000; Louie 2020) and Mike Widmer (2023) across the Reno area (>2,000 readings across the study area). Total uncertainty in the CBA by propagating errors for each correction is 0.076 mGal for readings within each data set and 0.634 mGal between data sets (Smith, 2024). Such uncertainty is much smaller than the magnitudes of the gravity anomalies we interpret, likely resulting in

variation of +/- 10 m for basin depths (Smith, 2024). The total CBA maps were contoured using the minimum curvature method.

Using published geologic maps (Rose, 1969; Soeller and Nielsen, 1980; Cordy and Mansour, 1985; Greene et al., 1991; Ramelli et al., 2011), we separated "basin" from "bedrock" to calculate Net Basin CBA maps, in the manner of Saltus and Jachens (1995). Bedrock areas included areas with exposed Mesozoic basement and Cenozoic volcanic units. Basin areas included Quaternary sedimentary units and (in Lemmon Valley) Miocene-Pliocene fluvial sediments of the Hunter Creek Formation. Maps of bedrock and basin distribution were built in ArcGIS. Bedrock CBA maps was generated using gravity readings within the bedrock area. These bedrock CBA maps were subtracted from the total CBA maps to generate net basin CBA maps that were used for all gravity modeling work.

Modeling

Two-dimensional gravity models were built from the net basin CBA maps following the approximate six (three in Lemmon Valley and three in TRIC) transects along which gravity and seismic data were collected for this study. Densities were estimated using density analysis of local lithologies on previous studies (Widmer, 2023). Basin depths were compared to depth-to-basement measurements from water well reports (see below) and were adjusted to fit well-derived basement depths. This procedure avoided the great uncertainties in interpreting thicknesses from gravity anomalies associated with the poorly known basin-fill densities. Pseudo-3D depth to basement maps were then generated using the properties from the 2d models for inputs. Finally, a depth-to-basement grid was generated from the from the map as an input to the community velocity model.

Seismic

Data Collection

Seismic data were collected in September-October 2023 using Fairfield 3-component Nodals borrowed from IRIS-PASSCAL. The Nodals were used to record ambient noise over a period of 2-15 hours for each line. Seven nodal arrays were deployed (Figure 2, Table 1, 3 in Lemmon Valley, 4 in TRIC) with 39-53 nodes per line, nodal spacing of 26-344 m, and total line lengths ranging from ~1 km to 22 km. Data from the Nodes are available via the IRIS website (https://ds.iris.edu/gmap/#network=5K&datacenter=IRISPH5&planet=earth), for Survey 5K. Each Nodal recorded vertical (GPZ), northing (GP1), and easting (GP2) components of ground velocity on the nominally 5 Hz internal geophones, sampled at 1000 Hz.

Table 1. Parameters for seismic surveys for this project.

Line No.	Spacing, m	No. Stations	Hours Recorded
1 all	138	47	2.0
1 long	138	42	12.0
2	73	49	15.0
3	55	48	3.0
5	26	39	2.5

7	344	43	7.5
8	175	53	8.0
9	313	44	13.0

ReMi analysis

Refraction Microtremor (ReMi) analysis was completed using 2dS+ and disper software version 2.1.7 from Terean. First, 30-minute data files were downloaded from the IRIS website for the vertical (GPZ) records. Thirty-minute records from each node were decimated and then concatenated into individual thirty-minute records for the entire survey line. These thirty-minute records were then combined into one large file for ReMi analysis. Each file was opened in 2dS+ and processed to generate a slowness-frequency plot, where we picked the basal surface representing the fundamental-mode Rayleigh phase-velocity dispersion curve. These picks were then brought into disper to build a 1D depth model of shear wave velocity to best fit the picks.

In ReMi analysis, depth of investigation is generally less than half of the line length (with the analysis at the center of the line), and resolution is a function of node spacing. Therefore, in addition to evaluation of each full line, the lines were also evaluated as a set of 12-node subarrays. 1D velocity models from the subarrays were then stitched together to form 2D velocity profile sections for each line. Note that due to the fairly wide node spacing, areas where the basin cover was thin were not able to be resolved.

HVSR analysis

Horizontal/vertical spectral ratio analysis (HVSR; e.g., SESAME, 2005; Bonnefoy-Claudet et al., 2006;) was applied to the nodal data as an additional method to evaluate depth to basement. HVSR analysis was completed using the 2dS+ software from Terean. First the thirty-minute records for all three nodal components (GPZ, GP1, and GP2) were downloaded. Each set of records were decimated and concatenated similar to the process for ReMi analysis. The horizontal (GP1 and GP2) were processed and averaged, and then these were divided by the vertical (GPZ) data, generating the H/V power-spectral ratio (HVPSR). The square root of the HVPSR then yielded the H/V amplitude-spectral ratio. This plot was evaluated from 0 Hz to 3-5 Hz. Peak values were picked for each node, with each of those picks used to calculate a basement depth.

Well logs

An additional check on modeled basin depths was to use logs from water wells available through the State of Nevada Department of Water Resources open data GIS hub (https://data-ndwr.hub.arcgis.com/). The website contains data and logs from over 100,000 water and geothermal wells throughout the state. In Lemmon Valley, over 200 well logs were evaluated along the three gravity/seismic transects, focusing on wells within ~1 km of each line. We also did a spot check looking for the deepest wells around Lemmon Valley. Forty-five of those were then incorporated into the final analysis. As TRIC is a smaller area, all of the well logs within the area were evaluated, with 25 incorporated into the final analysis. Evaluation consisted of

interpreting lithologic logs to estimate basement position. Most of the lithology descriptions consisted of generalized terms like rock, clay, gravel, hard rock, granite, dg (decomposed granite), weathered granite, etc. Basement was placed at the shallowest granitic, volcanic, or metamorphic unit within the lithologic log. Thus, at the TRIC the drilled depth to "rock" corresponds in most cases to the National Earthquake Hazard Map basin-depth parameter ***Z1.0***, the minimum depth to a shear-wave velocity of 1.0 km/s. Pancha et al. (2017) and Simpson and Louie (2020) reported rock velocities below and around the Reno-area basin. For logs that hit granitic basement in Lemmon Valley, depth to basement was at the intact granite and below the decomposed or weathered granite zone. In Lemmon Valley the drilled depth to "rock" more likely represents ***Z2.5***, the minimum depth to a shear-wave velocity of 2.5 km/s.

Results

Lemmon Valley

Gravity/Well log analysis

For Lemmon Valley, we initially modeled 2-d profiles along the three gravity transects, one north-south (transect A) and 2 east-west (transects B and C) (Figure 3). All models were built assuming 2.67 g/cc for basement density, and two-layered basins with a low density (1.6-1.9 g/cc) layer from the surface to ~150 m depth, and moderate density (2.0-2.3 g/cc) below ~150 m. Sediment densities were modified to allow basin thicknesses from gravity models to match depth to basement values from well logs. Many of the wells did not reach basement, and those are used as minimum thickness values within the gravity profiles.

North-south line

The north-south profile shows the deepest basement depths of the three 2D profiles (Figure 4). This line extends 20 km north from the northern flank of Peavine Mountain through Lemmon Valley and the Stead Airport and into the hills north of the airport across the southern flank of Freds Mountain. The profile has an upper basin density of 1.9 g/cc (down to 100 m), and lower basin 2.3 g/cc. The southern 5 km of the profile show a thin (<100 m) basin. Moving northward, the basin rapidly thickens to a maximum of 800 m ~7 km north of the southern end. The basin the shallows northward across a series of steps, ultimately terminating ~18 km n of the southern end of the profile.

Northern E-W profile

The northern E-W profile is ~14.5 km long, cutting through the central portion of the Lemmon Valley basin on the west and the shallow eastern Lemmon Valley subbasin in the east (Figure 5). The Lemmon Valley section occupies ~4 km of the line, starting ~3 km east of the west side of the line (located in Mesozoic basement rocks). The basin model is steeply sided, consistent with the north-striking faults mapped on each side of the basin (Soeller and Nielsen, 1980; Cordy and Mansour, 1985). The upper ~150 m of the model has a density of 1.92 g/cc, with 2.3 g/cc below, consistent with the north-south model. The deepest part of the Lemmon Valley basin on this side

is ~620 m, near the intersection with the N-S profile. The eastern part of the profile has much thinner basin sediments (generally less than 100 m thick), with a modeled average density of 1.6 g/cc. The lower density was required to allow the model to match well-based depth-to-basement measurements.

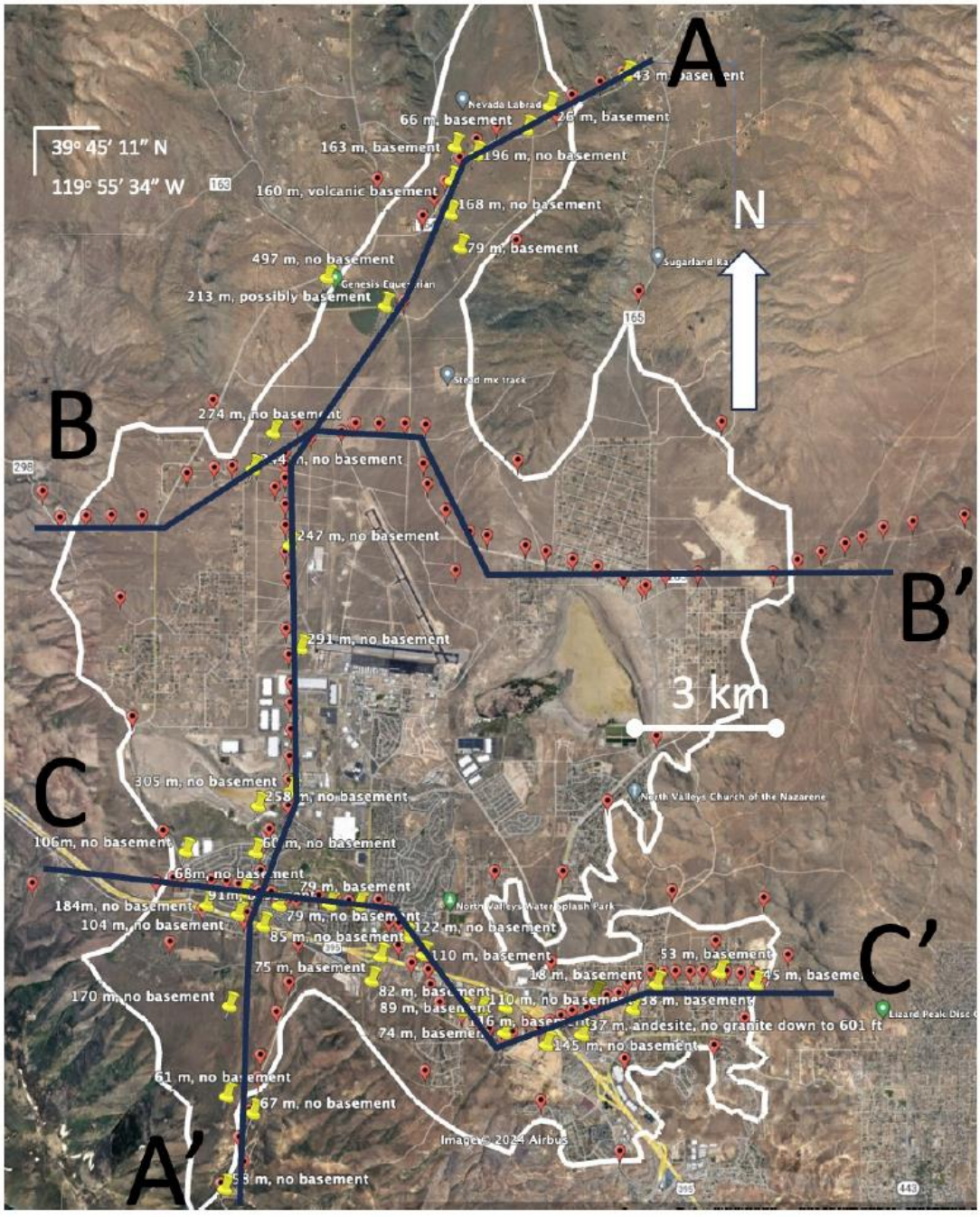

Figure 3. Google Earth image of Lemmon Valley area. Basin outline in white. Red circles are gravity stations from this study and yellow pins are wells with depth to basement. "No basement" indicates the well did not penetrate basement at TD. Lemmon Valley gravity profile lines are in black. Figure from Smith (2024).

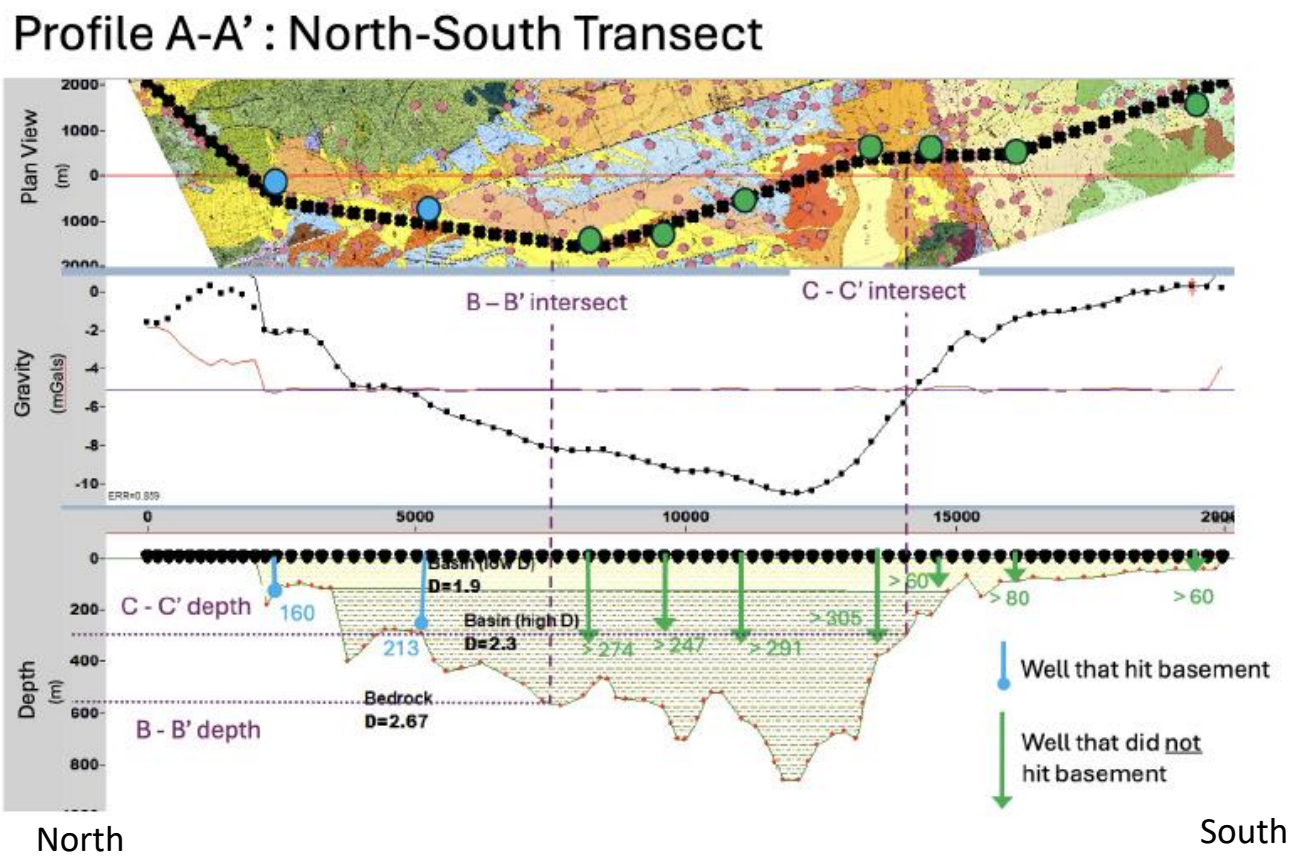

Figure 4. Gravity model for line A-A'. Top panel is a geologic strip map. Green units are Mesozoic basement, light blue is Miocene sediments (included with basin deposits), and yellow and orange units are Quaternary sediments. Circles show locations of wells along the line used as control. Blue circles indicate wells that penetrated basement and green circles are wells that did not reach basement. Middle panel shows gravity data (black circles), gravity model (black line), and residual (red line), and bottom panel shows 2d density model, including depth of well penetrations and depth at the intersections with lines B and C. Maps from Soeller and Nielsen (1980), Cordy and Mansour (1985), and Ramelli et al. (2011). Figure from Smith (2024).

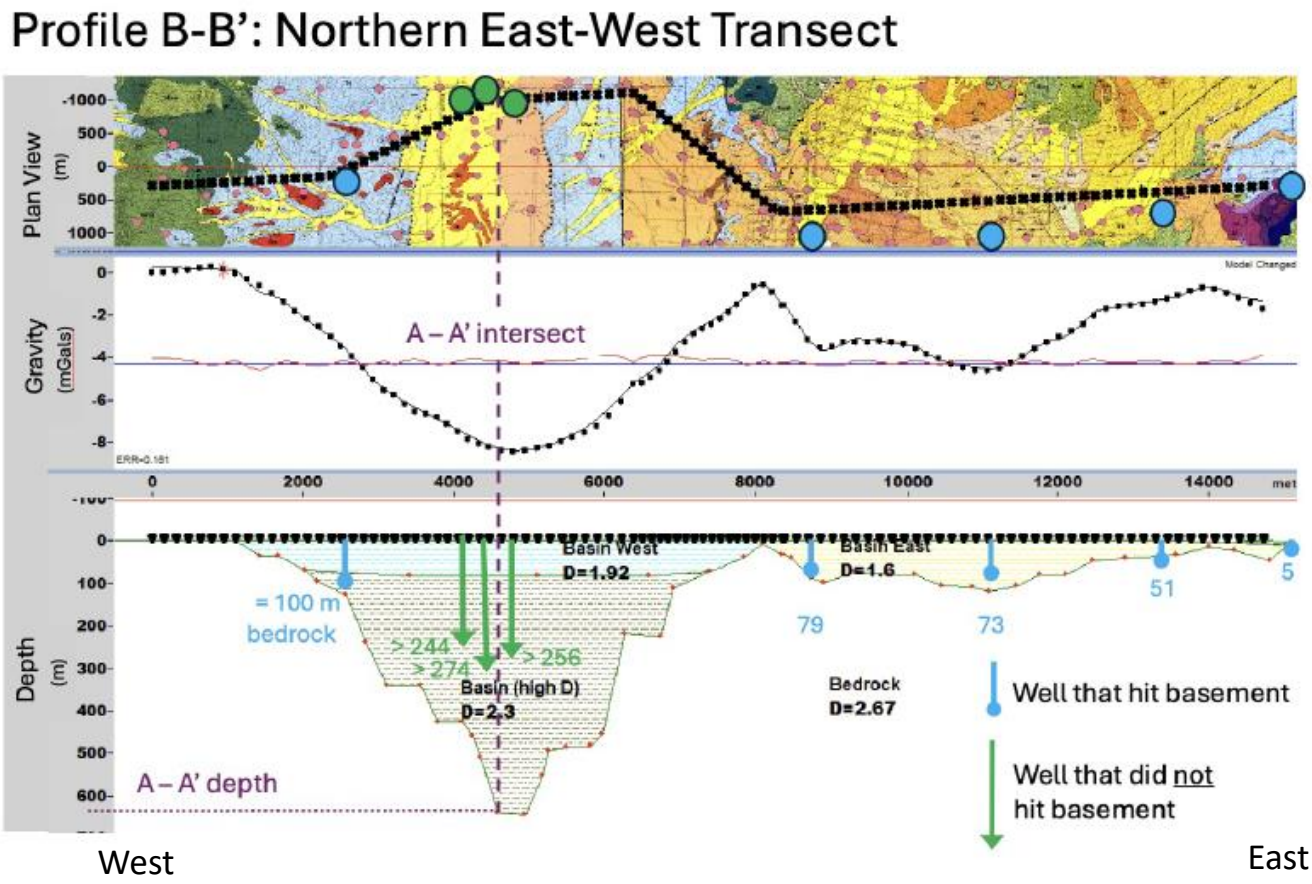

Figure 5. Gravity model for line B-B'. Top panel is a geologic strip map. Green units are Mesozoic basement, purple is Oligo-Miocene volcanic rocks, light blue is Miocene sediments (included with basin deposits), and yellow and orange units are Quaternary sediments. Circles show locations of wells along the line used as control. Blue circles indicate wells that penetrated basement and green circles are wells that did not reach basement. Middle panel shows gravity data (black circles), gravity model (black line), and residual (red line), and bottom panel shows 2d density model, including depth of well penetrations and depth at the intersections with line A. Maps from Soeller and Nielsen (1980) and Cordy and Mansour (1985). Figure from Smith (2024).

Southern E-W profile

The southern E-W profile is 12 km long, crossing the southern fringe of the Lemmon Valley basin and Golden Valley basin along the US-395 corridor (Figure 6). The depth to basement is mostly less than 100 m, with the exception of the central part of Lemmon Valley, with a depth of nearly 300 m just west of the intersection with the north-south line. As with the northern E-W line, this line shows Lemmon Valley to be a steep-sided, likely fault-bounded, basin. However, in this profile the basin is only 2 km wide, considerably narrower than along the northern E-W transect. Basin density is modeled as 1.92 g/cc throughout.

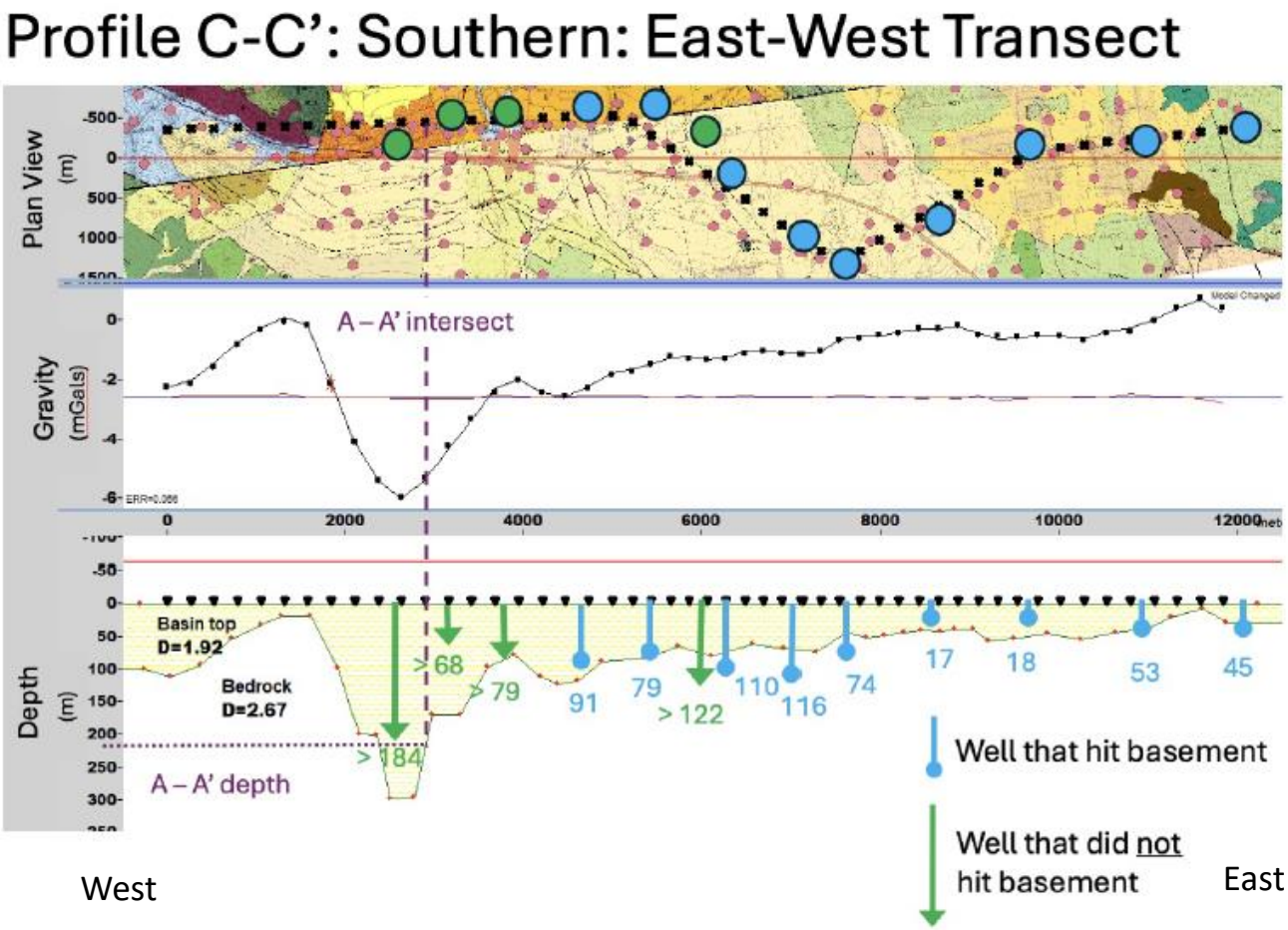

Figure 6. Gravity model for line C-C'. Top panel is a geologic strip map. Green units are Mesozoic basement, purple is Oligo-Miocene volcanic rocks, light blue is Miocene sediments (included with basin deposits), and yellow and orange units are Quaternary sediments. Circles show locations of wells along the line used as control. Blue circles indicate wells that penetrated basement and green circles are wells that did not reach basement. Middle panel shows gravity data (black circles), gravity model (black line), and residual (red line), and bottom panel shows 2d density model, including depth of well penetrations and depth at the intersections with line A. Maps from Soeller and Nielsen (1980), Cordy and Mansour(1985), and Ramelli et al. (2011). Figure from Smith (2024).

A depth-to-basement map was constructed from the total CBA map (Figures 7-11) using a linear regression analysis between modeled basin depths and net basin CBA values (Figure 8). The regression shows two linear trends, a basin thickness increase of 20 m per decrease in mGal within the shallow (low density) part of the basin, and an increase of ~95 m in basin thickness per mGal decrease in the deeper (high density) part of the basin. These equations were applied to the net basin CBA map to produce a depth to basement (or basin thickness) map (Figure 11). This map shows Lemmon Valley as an elongate ~north trending basin that is ~4 km wide and has its deepest point of ~850 m in the south-central part of the basin, near Silver Lake. To the north,

the basin shallows to a depth of ~300-400m. The southern portion of our basin outline along the US-395 corridor is relatively shallow, with the basin thickness generally less than 100 m. In the eastern part of the study area there is also a smaller NE-trending 4 km-long by 2 km-wide sub-basin in the Swan Lake area that is ~300-400 m deep. Finally, outside of the Lemmon Valley study area, there are several other deep (800-900 m) basins apparent, including White Lake basin to the west and Hungry Valley or northern Spanish Springs basin to the east-northeast.

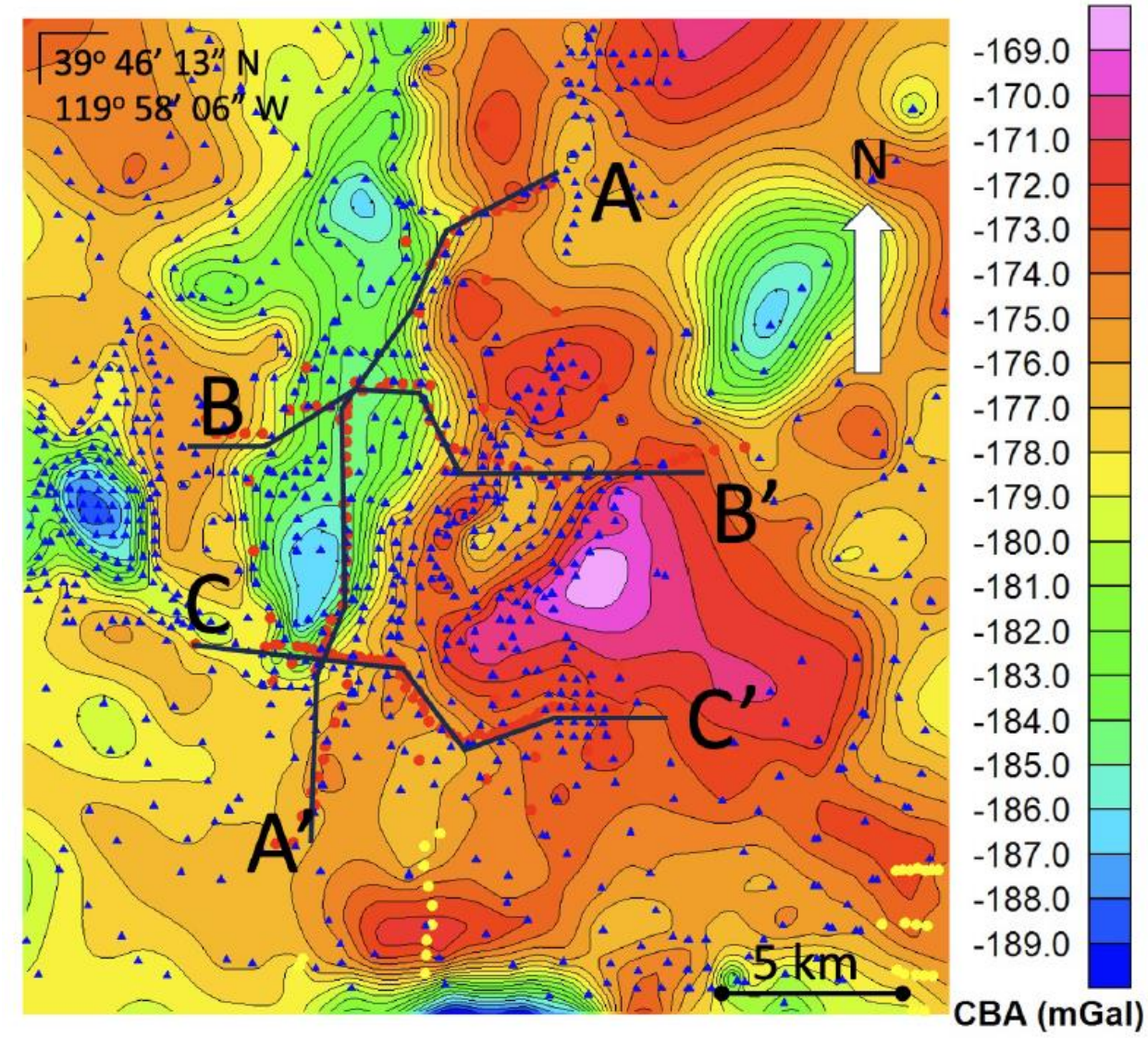

Figure 7. Total CBA map for the Lemmon Valley area. Contour interval is 1 mgal.
Red circles are gravity measurements from this study. Yellow circles and blue triangles are measurements from previous studies. Black lines are gravity profiles. Figure from Smith (2024).

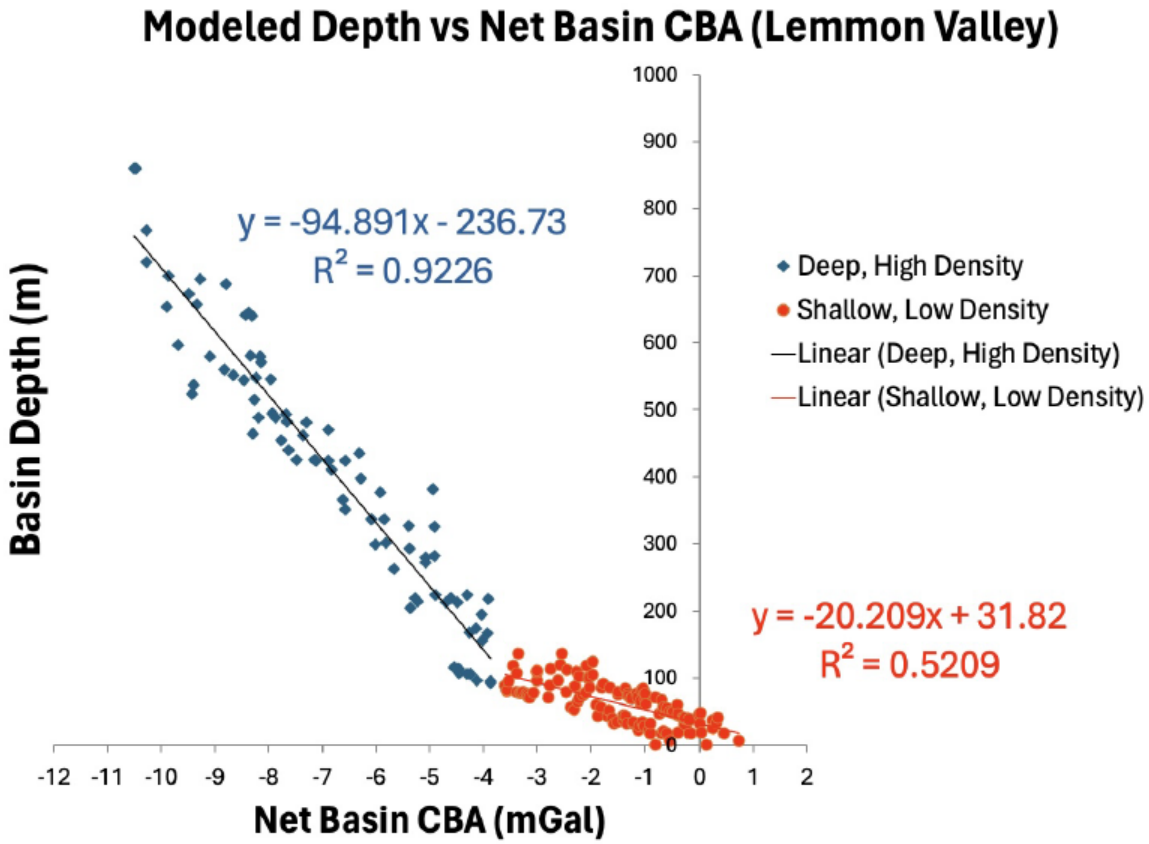

Figure 8. Linear regression analysis showing relationship between Net Basin CBA and modeled depth from 204 data pairs across three 2d models in Lemmon Valley. These relationships were used to extrapolate Net Basin CBA map to a depth to basement map. Figure from Smith (2024).

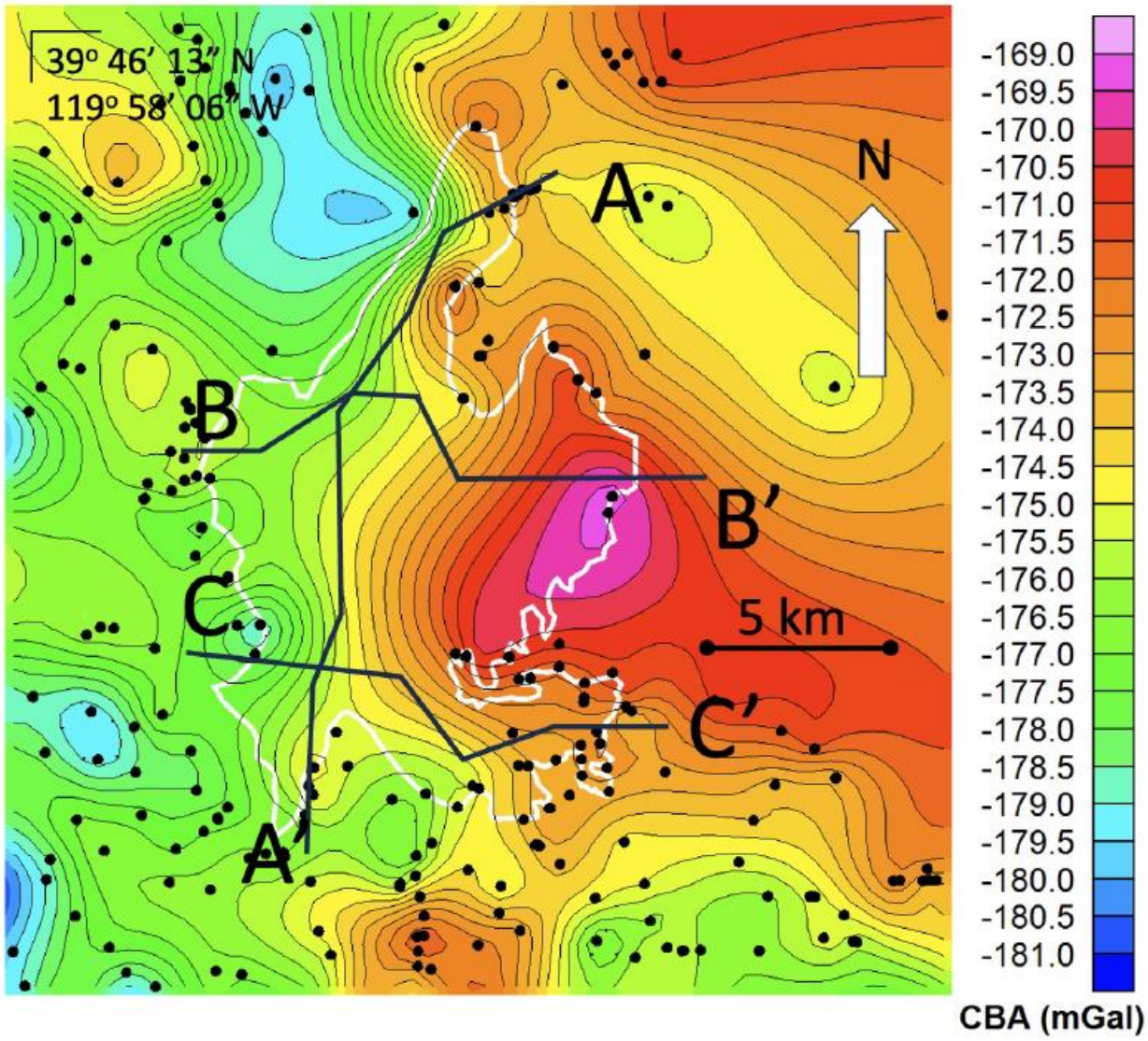

Figure 9. Bedrock CBA map for the Lemmon Valley area built using only the stations Located on bedrock (black circles). Contour interval is 0.5mgal. Figure from Smith (2024).

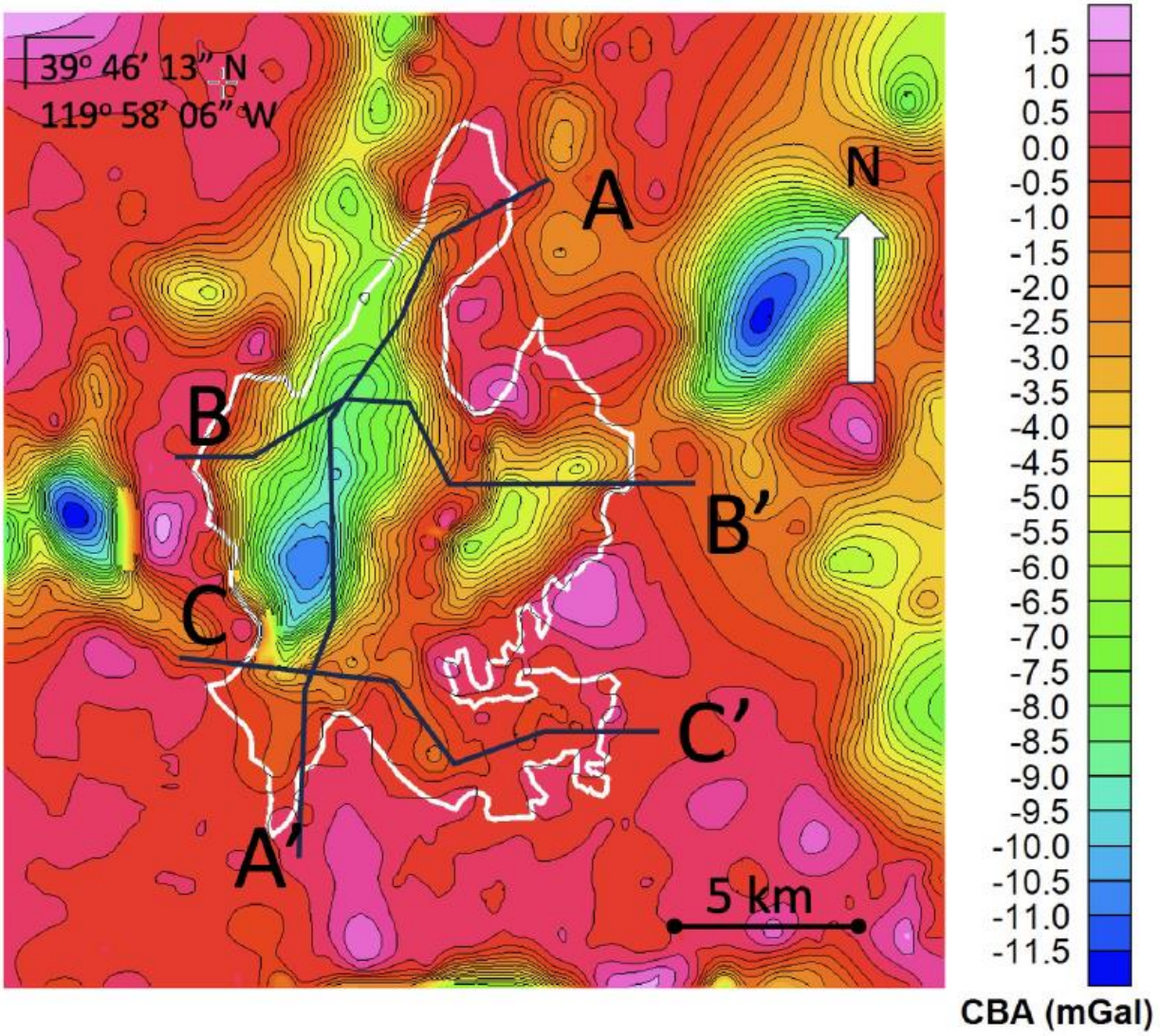

Figure 10. Net basin CBA map for the Lemmon Valley area. Map was calculated by subtracting the Bedrock CBA map from the Total CBA map. Contour interval is 0.5 mgal. Figure from Smith (2024).

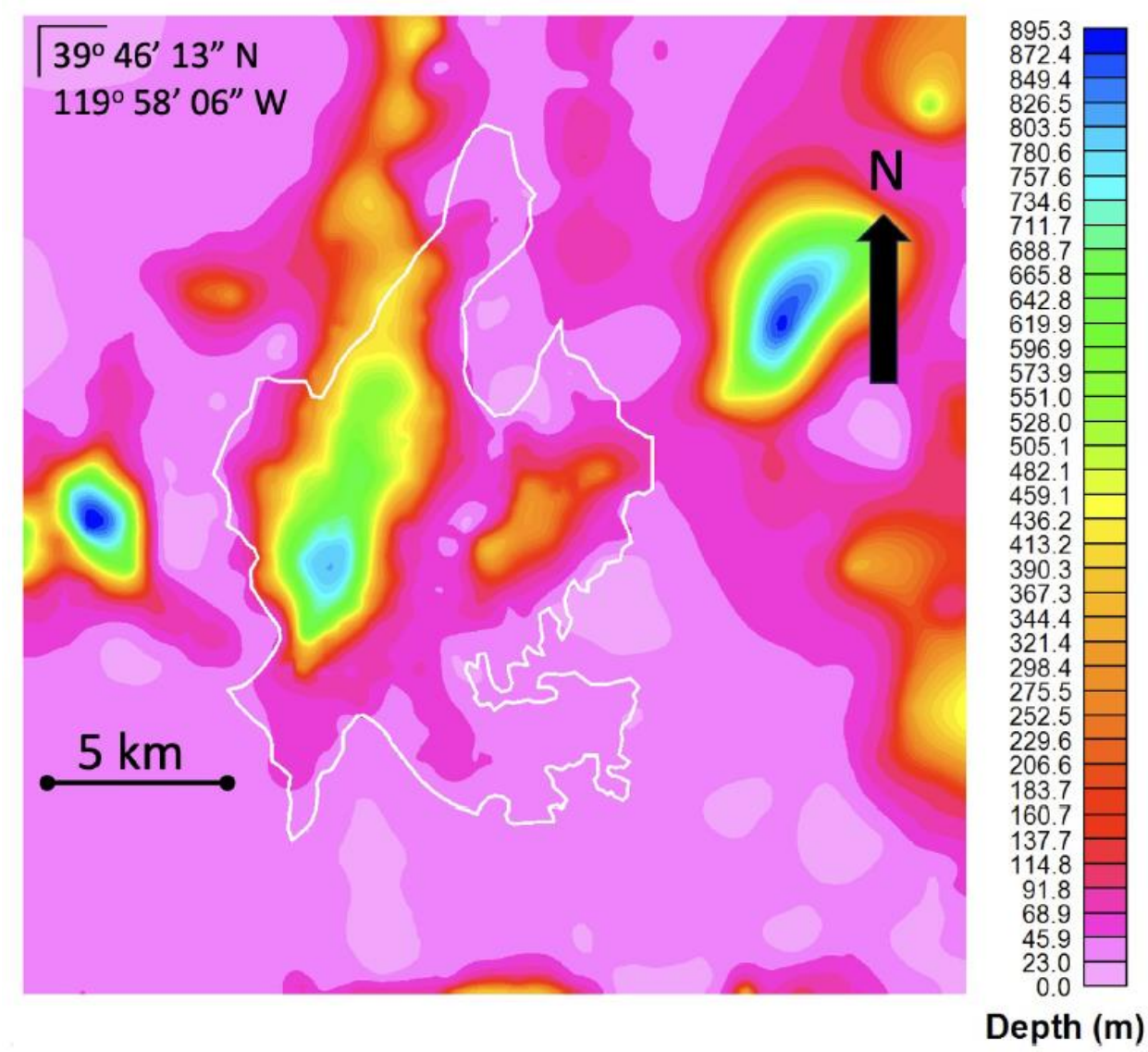

Figure 11. Depth to basement map for the Lemmon Valley area. Figure from Smith (2024).

Seismic methods

We collected seismic data for ReMi and HVSR analysis along three transects in Lemmon Valley (Figure 2), following the three 2D gravity transects. Fairfield 3-component seismic Nodals were deployed for each transect and the collected ambient noise (traffic, wind, trains, planes, industrial) for a period of at least three hours. The resulting data were processed and analyzed using the 2dS+ software from Terēan. The results from each line are described below.

North-south line (Line 9)

Line 9 had 44 nodes deployed across 13.5 km (north-south) with an average spacing of 313 m. Nodes were deployed on Sept. 29, 2023 and they recorded noise for 13 hours, resulting in 26 30-

minute records for analysis. For ReMi analysis the data were divided into 33 sub-arrays with 12 nodes per array. Each sub-array was analyzed to generate a 1D velocity profile, ad those profiles were then stitched together to form a 2D Vs model (Fig. 12). On this model (and the other ReMi models) depths to shear wave velocities of 1 km/s (Vs 1.0) and 2.5 km/s (Vs 2.5) are plotted, with Vs 2.5 acting as a proxy for depth to basement. The model shows the basin gradually deepening southward (the Vs 2.5 line), from 400 m depth in the north to ~700 m in the south. This is followed father south by a step up in basin depth to ~500-600 m. The Vs1.0 line deepens from the surface in the north to a depth of 300 m across much of the basin, shallowing to ~225 m depth in the south.

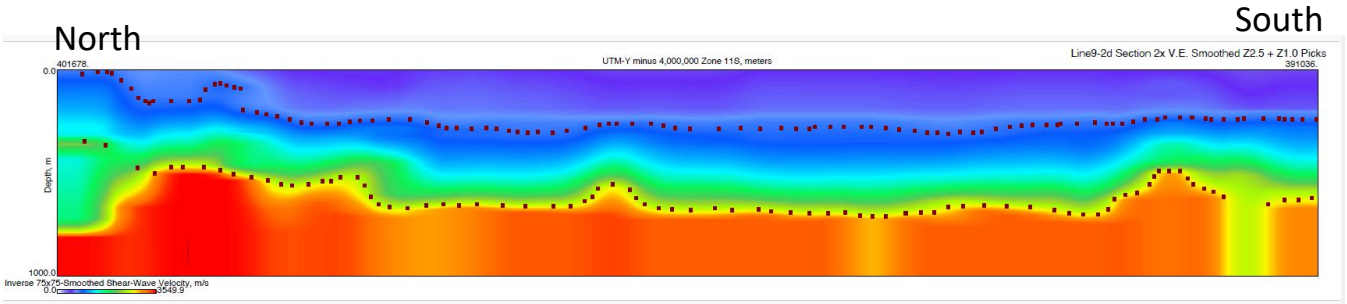

Figure 12. ReMi-derived 2d Vs profile along line 9 in Lemmon Valley. Upper set of dots represents depth to a shear wave velocity of 1.0 km/s. Lower set of dots is depth to shear-wave velocity of 2.5 km/s and also serves as a proxy for depth to basement.

HVSR analysis for line 9 (Figure 13) was calculated by averaging the two horizontal nodal components and dividing by the vertical component. The result of those calculations is a plot of distance vs. frequency (increasing downward from 0 to several Hz), with the colors representing the smoothed average power (amplitude) of the spectral ratios. Then one or more peak amplitudes are picked for each track. These values can then be converted to a quarter-wavelength estimate of basin thickness by dividing the average estimated Vs for the basin fill by the peak frequency and dividing that value by 4. The depth to basement values determined by HVSR analysis are similar to those from ReMi (Figure 14), with basin depth starting at ~400 m in the north, deepening toward the south to ~700 m and then shallowing to ~550 m. In the HVSR analysis, the deepest part of the basin is shifted ~3 km northward relative to the deepest part of the basin determined from gravity and ReMi. For line 9 we used 1100 m/s as the average Vs for the basin, but this likely varies along the transect, which may explain the discrepancies between HVSR and the other analytical techniques.

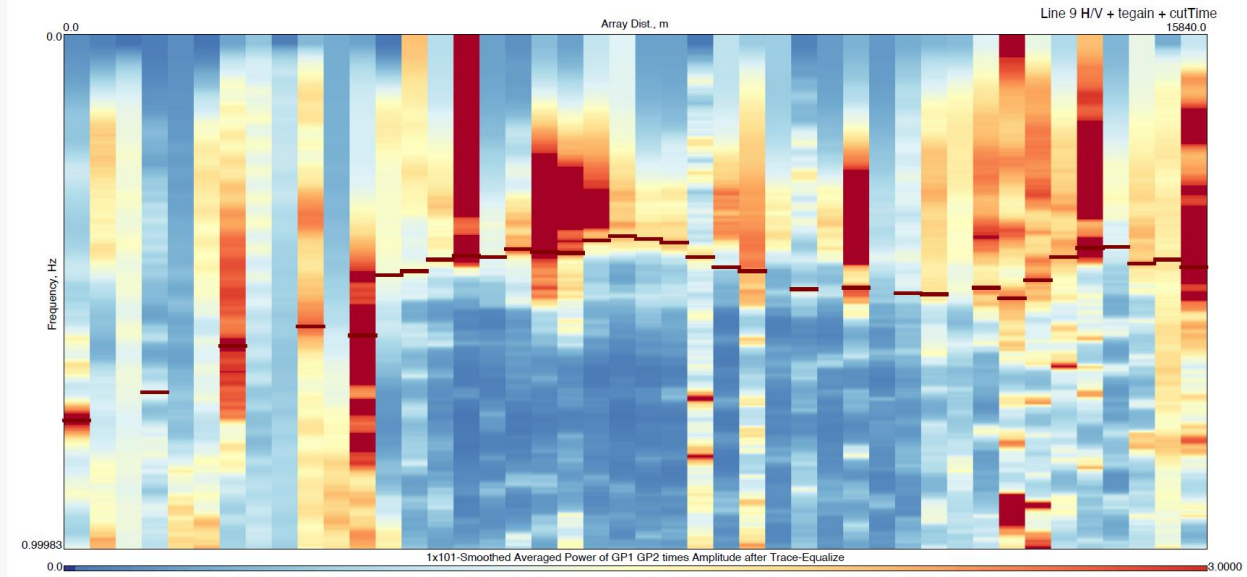

Figure 13. Line 9 HVSR analysis, plotting increasing frequency (y-axis) versus distance along the array (y-axis). Picks for peak power along the line are shown by the red bars.

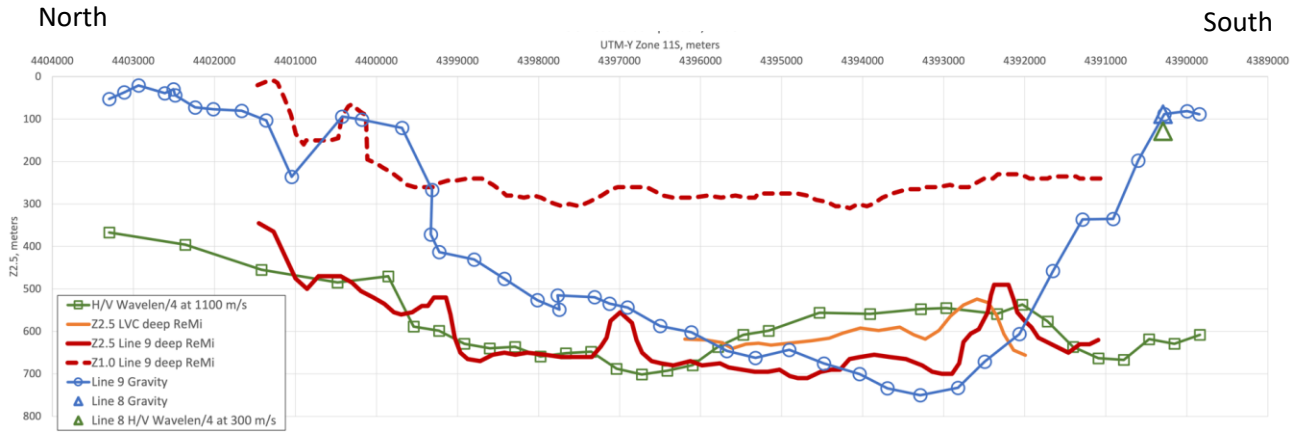

Figure 14. Comparison of depth to basement for line 9 (north-south) in Lemmon Valley. Models are derived from gravity (blue circles), two types of ReMi analysis (red and orange lines), and HVSR analysis (green squares). Also includes depth to Vs 1.0 km/s derived from ReMi analysis (dashed red line). Plotted north (left) to south (right) and scaled at 5x vertical exaggeration.

Northern east-west line (Line 7)

Line 7 is the northern of the two east-west lines in Lemmon Valley, extending 14.8 km (east-west) with 43 nodes and an average node spacing of 353 m. Nodes were deployed on Sept. 23, 2023 and they recorded noise for 8 hours, resulting in 16 30-minute records for analysis. This line crosses the northern portion of Lemmon Valley in the west along the northern boundary of Stead airport, then continues east, passing north of Swan lake and ending in bedrock west of

Hungry Valley. For the ReMi analysis we generated 32 12-node subarrays to develop a 2D Vs profile. The western 12 subarrays, with midpoints between 1 and 6 km east of the western end of the line showed basin depth increasing from ~250 m to ~450 m (Figure 15).

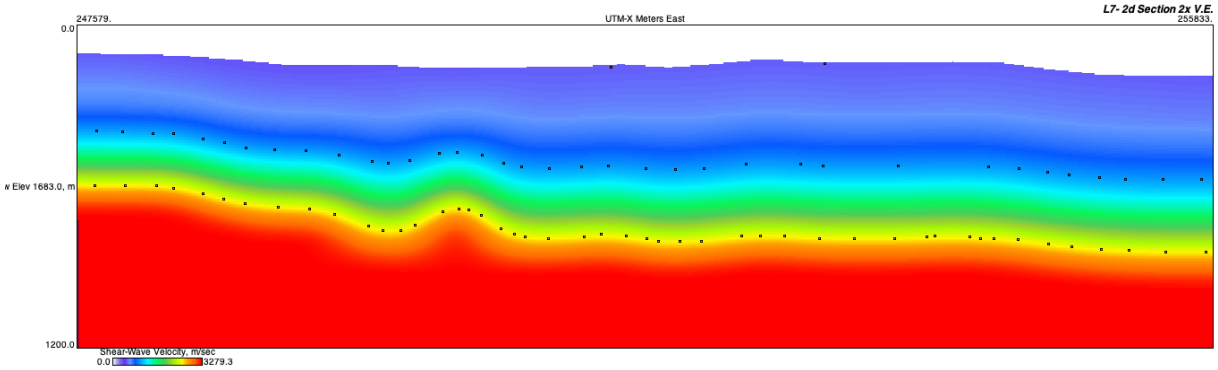

Figure 15. Deep ReMi shear-wave-velocity cross section along the western portion of Line 7, running west to east. Black squares show picks of Z1.0 (medium blue color) and Z2.5 (yellow color).

Line 7 HVSR analysis (Figure 16) has an initial decrease in peak frequency toward the east as it passes across the core of Lemmon Valley, followed by an increase in peak frequency as the line went across the eastern boundary of Lemmon Valley and then another decrease at the eastern end of the line in the northeastern Lemmon Valley subbasin. Depth conversion for this line was challenging as average basin velocity values were highly variable with higher values in the deepest parts of Lemmon Valley basin and lower values on the shallower sides of the basin. Depths were calculated using low (360 m/s) and high (900 m/s) average basin Vs (Fig. 17). The low Vs depths match the shallow parts of the basin, on the ends and in the center of line 7. The higher Vs depths are closer to the gravity derived-depths for the deeper parts of line 7, including the main Lemmon Valley basin in the west and the northeastern Lemmon Valley subbasin in the east.

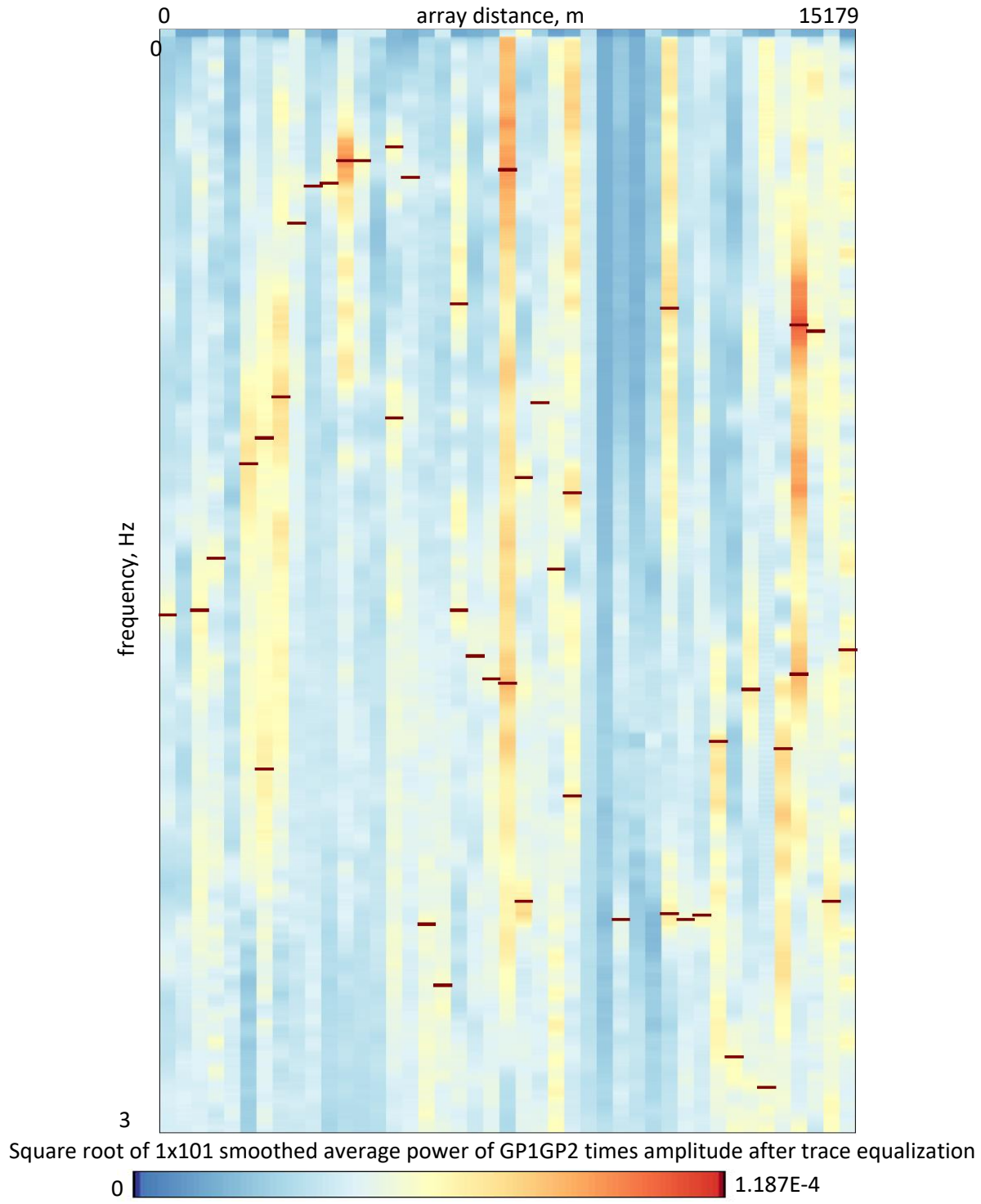

Figure 16. Line 7 HVSR analysis, plotting increasing frequency (y-axis) versus distance along the array (y-axis). Picks for peak power along the line are shown by the red bars.

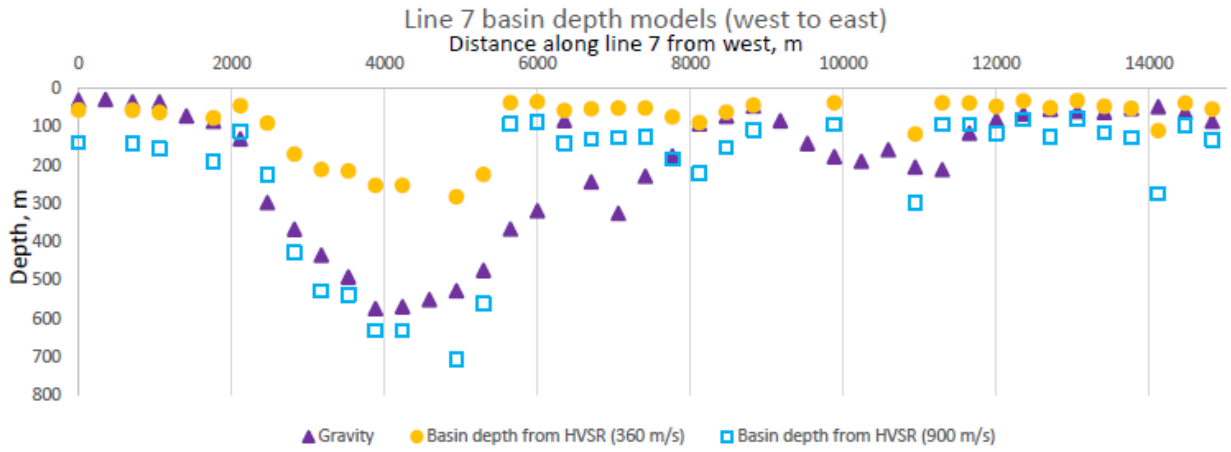

Figure 17. Comparison of depth to basement derived from gravity (triangles) and HVSR analysis assuming average basin Vs of 360 m/s (circles) and 900 m/s (open squares) for line 7 in Lemmon Valley. Plotted west (left) to east (right) and scaled at 5x vertical exaggeration.

Southern east-west line (Line 8)

Line 8 is the northern of the two east-west lines in Lemmon Valley, extending 9.3 km (east-west) with 53 nodes and an average node spacing of 175 m. Nodes were deployed on Sept. 30, 2023 and they recorded noise for 8 hours, resulting in 16 30-minute records for analysis. The line follows the US-395 corridor from south of Silver Lake, to approximately Lemmon Drive, where the profile continues east across the southern end of Golden Valley. The general shallow depth to basement along line 8 and the wide nodal spacing resulted in simple ReMi analysis not determining Quaternary basin properties, as the basin thickness was generally below vertical resolution from the ReMi analysis. The Line 8 HVSR analysis (Figure 18) generally shows an increase in peak frequency eastward across the line, consistent with a decrease in depth to basement toward the east. Since this line does not cross over the deepest part of the basin, we used lower average basin Vs values for the analysis, with one realization at 300 m/s and one at 500 m/s. Additionally, for some of the nodes we picked two peak amplitudes as it was unclear in the HVSR spectral plot which was correct. All of the HVSR plots show a deeper basin in the western 1.5 km, with the basin shallowing to 50-100 m depth across the remainder of line 8. The western basin (which is the southern end of Lemmon Valley basin depths vary from 125 m (at 300 m Vs) to 275 m (at 500 m Vs). The values using 500 m/s Vs are more consistent with depth estimates from gravity (Figure 19). However, these values tend to overestimate depth across the rest of line 8, where 300 m/s Vs values produce basin depths similar to the 40-75 m depth range from gravity analysis.

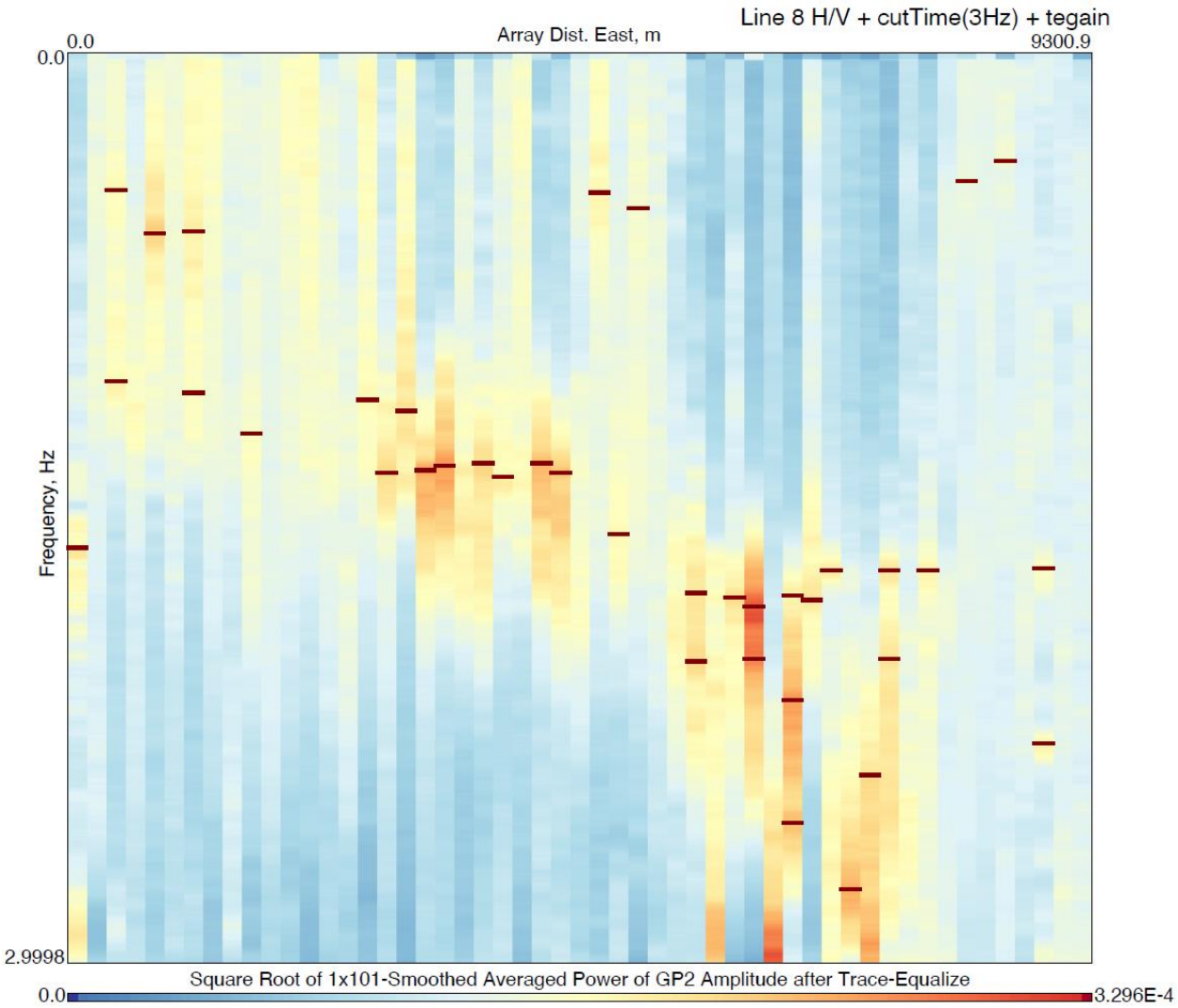

Figure 18. Line 8 HVSR analysis, plotting increasing frequency (y-axis) versus distance along the array (y-axis). Picks for peak power along the line are shown by the red bars.

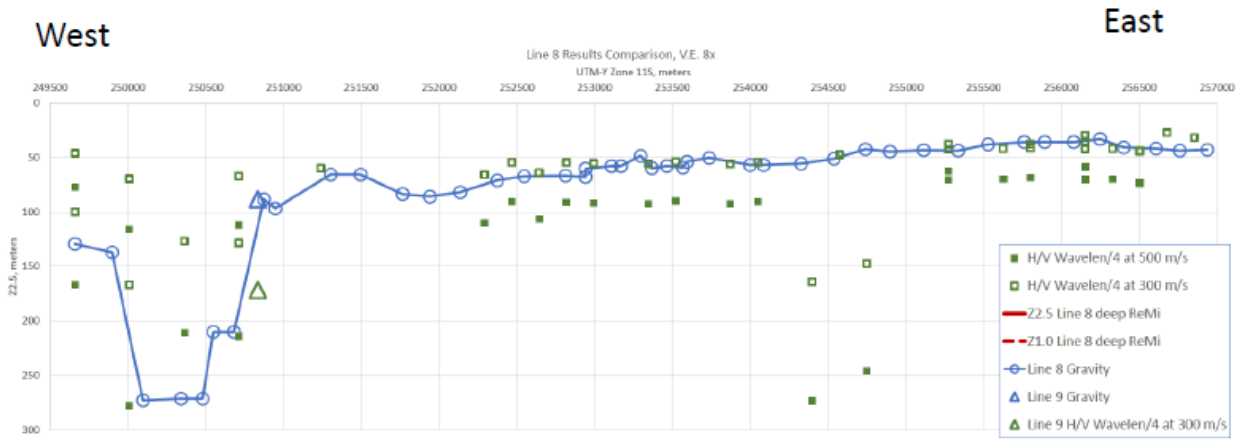

Figure 19. Comparison of depth to basement for line 8 (northern west-east) in Lemmon Valley. Models are derived from gravity (blue circles) and HVSR analysis (green squares). Plotted west (left) to east (right) and scaled at 8x vertical exaggeration.

TRIC

Gravity/Well log analysis

Overall, the gravity data from TRIC were more difficult to interpret and model coherently compared to those from Lemmon Valley. This is due to the very different geology in TRIC relative to Lemmon Valley. TRIC is dominated by Cenozoic volcanic units, including the >1km thick Miocene Pyramid mafic sequence in the north and east, and the Clark Mountain andesitic volcano on the southwest (Figures 20 and 21). The TRIC "basin" has a smaller area, generally extending north-south, with an elongated strip in the north where the Truckee River and Olinghouse fault cut through the basin. Below the Miocene-Pleistocene volcanics are a variety of lithologies, including diatomite-dominated lacustrine sediments, intermediate volcanic and volcaniclastic units, and ash-flow tuff-filled paleochannels (e.g., Schwartz, 2001; Schwartz and Faulds, 2004; Faulds et al., 2008; Sturmer and Faulds, 2018). These units all sit atop Mesozoic igneous and metamorphic basement.

Saltus and Jachens (1995) used regionally sparse gravity data to estimate depths to Mesozoic basement of up to 2 km, possibly corresponding to ***Z2.5***. The Tertiary sediments and volcanics we are considering to be basement for this project are more likely to correspond to ***Z1.0***. The variety of densities of the sub-mafic volcanic units and unequal distribution of those units makes it difficult to extrapolate 2D gravity lines to generate a pseudo-3d depth to basement map (Figure 22). Therefore, below we present our preferred models for the three gravity lines, followed by a depth to basement map that we calculated from 25 well-derived depth to basement values.

Gravity models were built for three profiles across TRIC (Figure 23), approximately following seismic profile lines. Profile A-A' (Figure 24) is across the Truckee River corridor on the west side of TRIC. The gravity model shows a narrow and shallow (20 m) Quaternary basin across the river set into dense Miocene volcanic units. Below the Miocene volcanic we model less dense sedimentary units, interpreted as a northern extension of the diatomaceous and fluvial sediments of Chalk Hills that are exposed several km to the southwest (e.g., Schwartz, 2001; Schwartz and Faulds, 2004). Older volcanic and metamorphic basement is interpreted below the sediments. Profile B-B' (Figure 25) trends SSE across the core of TRIC. B-B' also contains a relatively shallow Quaternary basin (up to 60 m deep), with Miocene volcanic units below. However, on the south end of this profile we model a denser unit below the volcanics, which is perhaps an Oligo-Miocene welded-tuff paleochannel (e.g., Henry, 2008; Henry and Faulds, 2010; Henry and John, 2013) or a dense mineralized zone. Profile C-C' (Figure 26) cuts SW-NE across TRIC. The model for profile C-C' has Quaternary deposits (up to ~100 m thick) thickening across the core of the basin and again to the SW. Miocene volcanic units are interpreted below the Quaternary sediment.

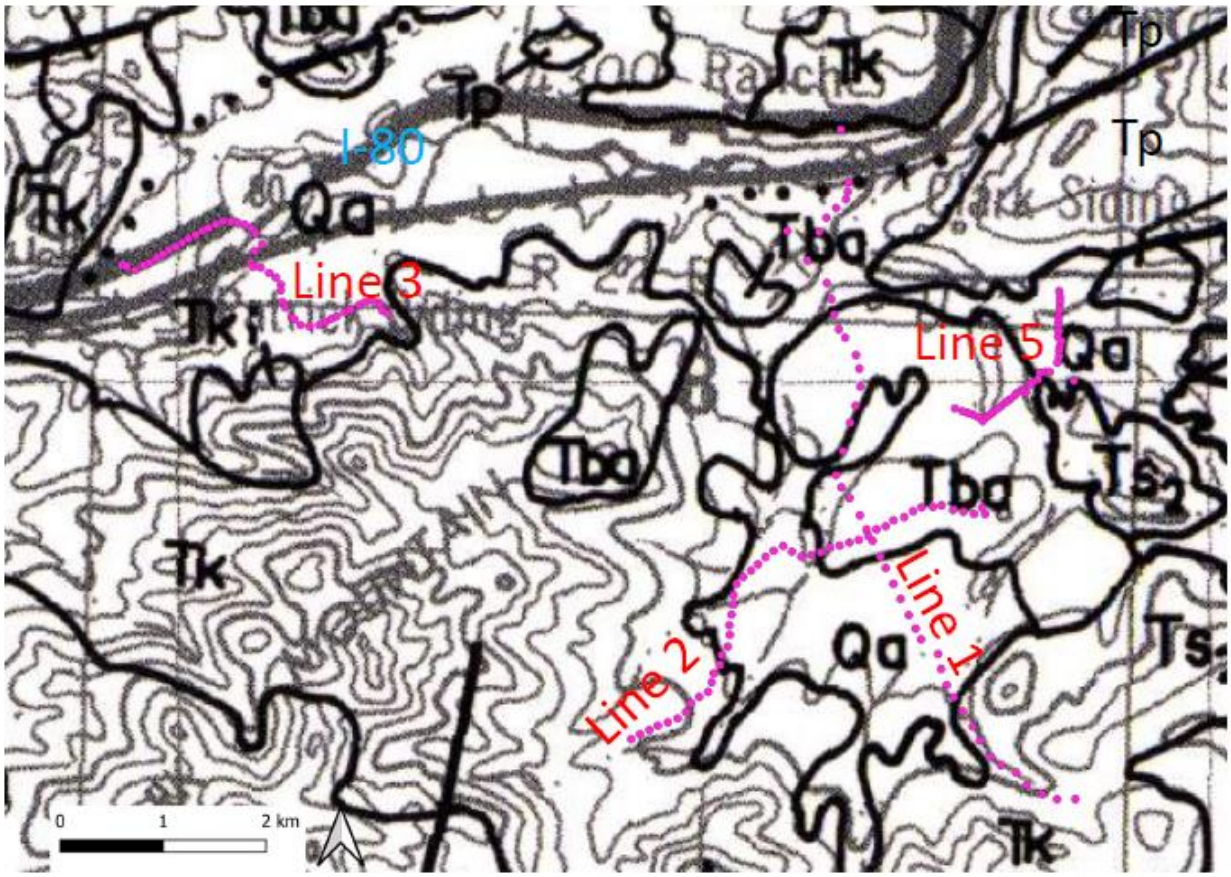

Figure 20. Geologic map showing seismic lines acquired in TRIC. Small pink circles indicate seismic node locations. Qa, Quaternary alluvium; Tba, Miocene basalt and andesite flows; Tk, Miocene Kate Peak Formation (dacite flows, breccias, and lahar deposits); Tki, Miocene intrusive rocks (dacite) of the Kate Peak Formation; Tp, Miocene Pyramid sequence (basalt, basaltic andesite, and andesite flows, flow breccias, and lahar deposits with local tuff, sandstone, and diatomite); Ts2, Miocene lacustrine and fluvial tuffaceous shale, diatomite, and sandstone. Map from Greene et al. (1991).

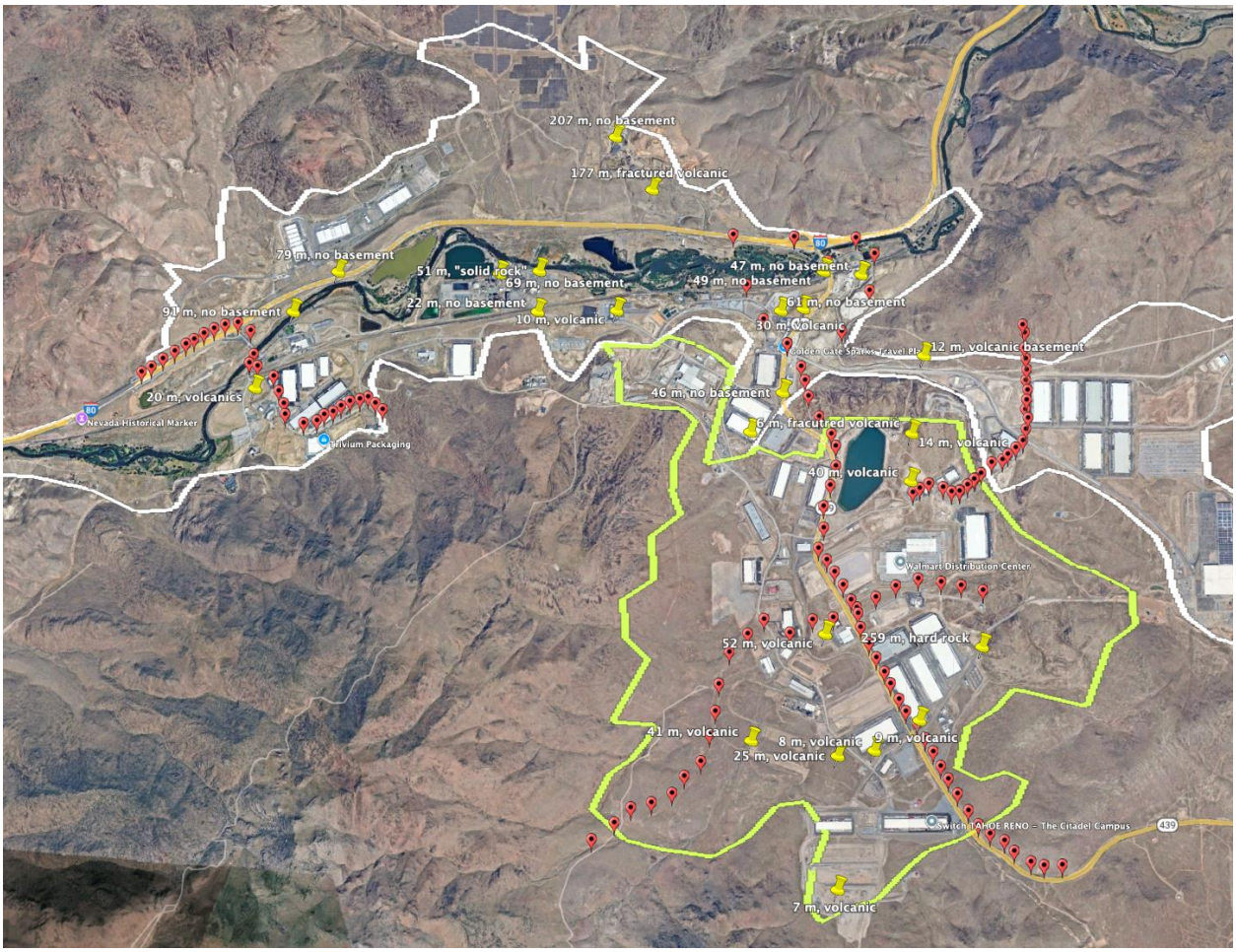

Figure 21. Google Earth image covering approximately the same area as Figure 20. Red darts indicate seismic node locations. Yellow pins indicate water wells used in our basement depth map.

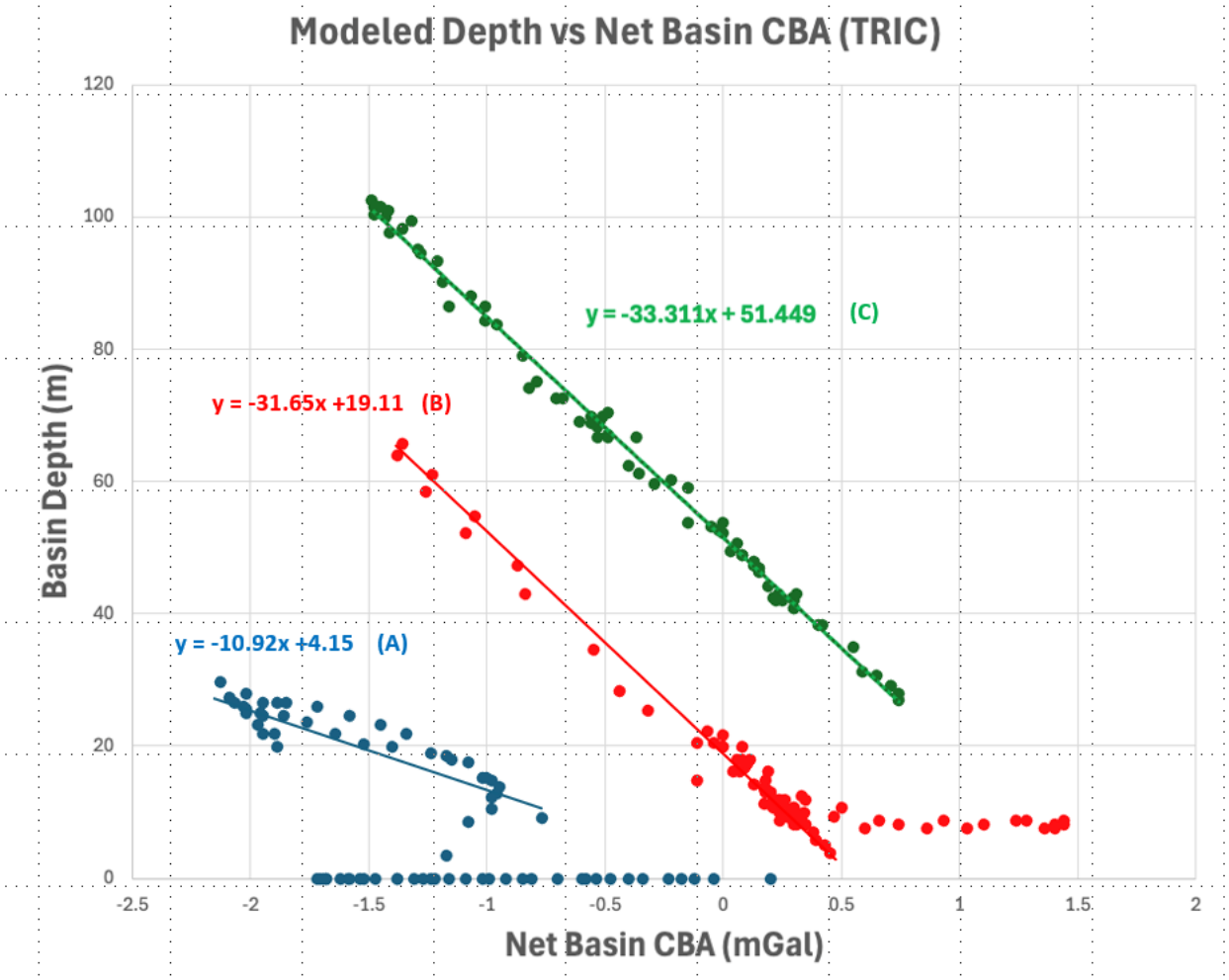

Figure 22. Linear regression analysis showing relationship between Net Basin CBA and modeled depth from three 2d models in TRIC. Complexities in the bedrock below the Quaternary basin result in these three very different profiles. These differences preclude a simple conversion from Net CBA to basin depth. Therefore, we used a contour map of depth to basement from well logs as an alternative.

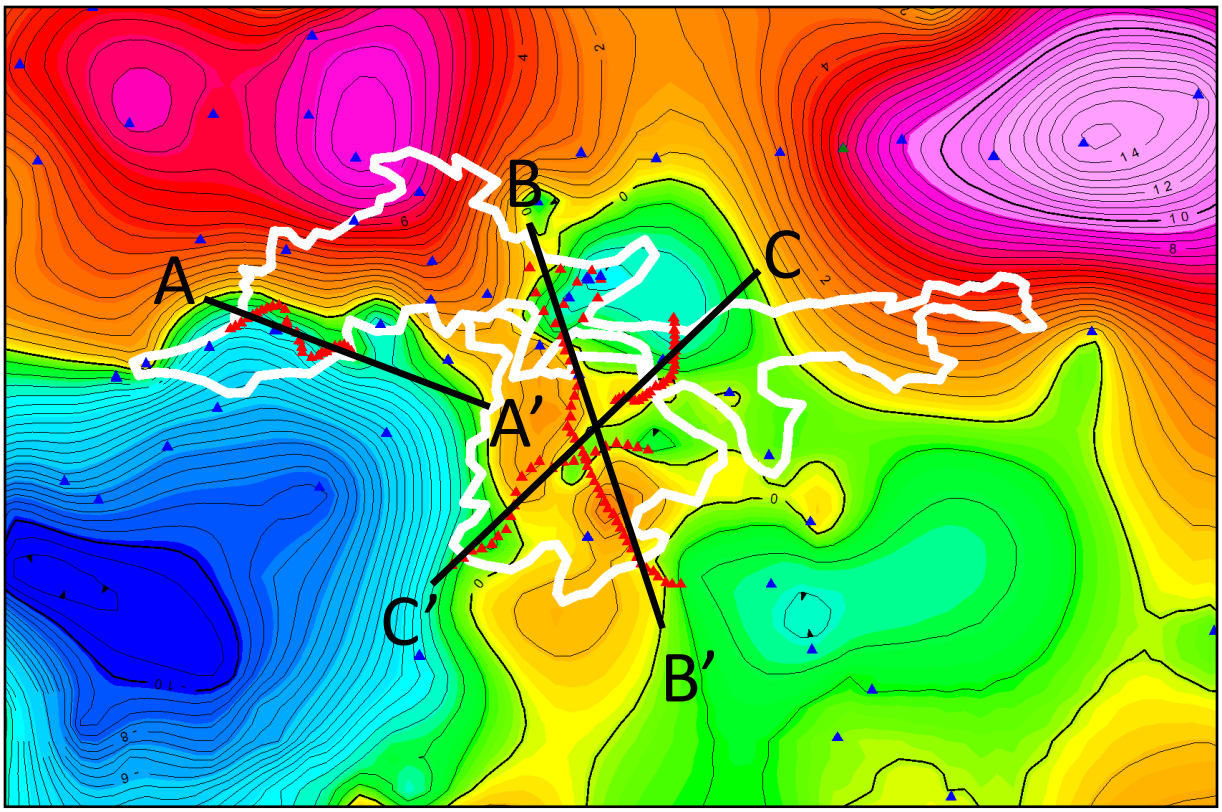

Figure 23. Net basin CBA map for TRIC and the surrounding area. Bold contours are 10 mgal and contour interval is 0.5 mgal. Cool colors (green and blue) represent negative values down to -11mgal in the southwest. Warm colors (yellow to pink) represent positive values up to 14.5 mgal in the northeast. North is up. White outline indicates approximate basin outline for TRIC. Black lines are lines modeled for gravity. Red triangles are gravity locations for this study and blue triangles are gravity locations from previous studies included in this analysis.

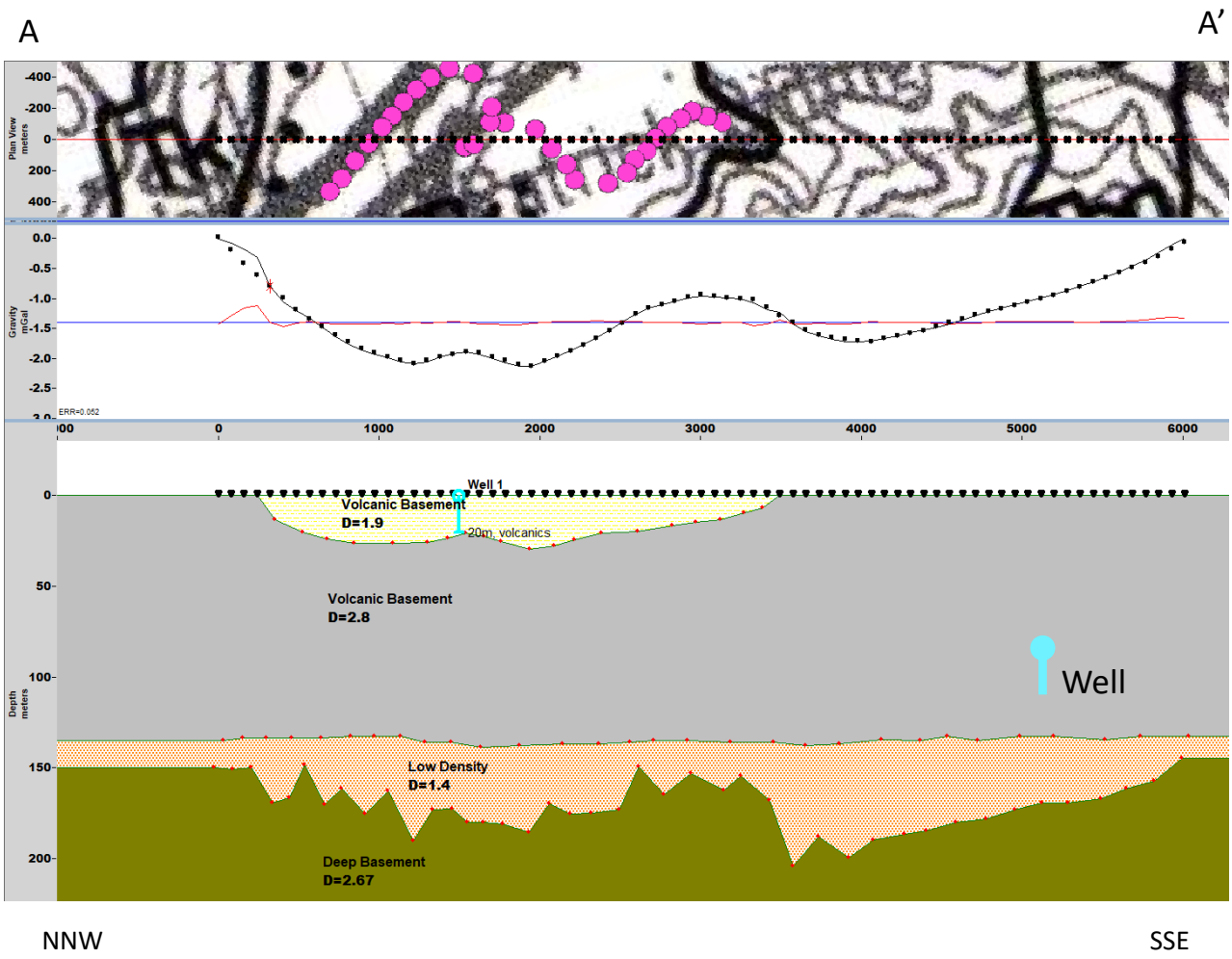

Figure 24. Gravity model for line A-A'. Top panel is a geologic strip map from Figure 20. Middle panel shows gravity data (black circles), gravity model (black line), and residual (red line). Bottom panel shows preferred 2d density model, including control on thickness of Quaternary basin from one well (light blue line). Low density unit interpreted as a continuation of diatomite-dominant lacustrine and fluvial sediments of Chalk Hills described on the southwest side of Clark Mountain by Schwartz (2001) and Schwartz and Faulds (2004). Map from Greene et al. (1991).

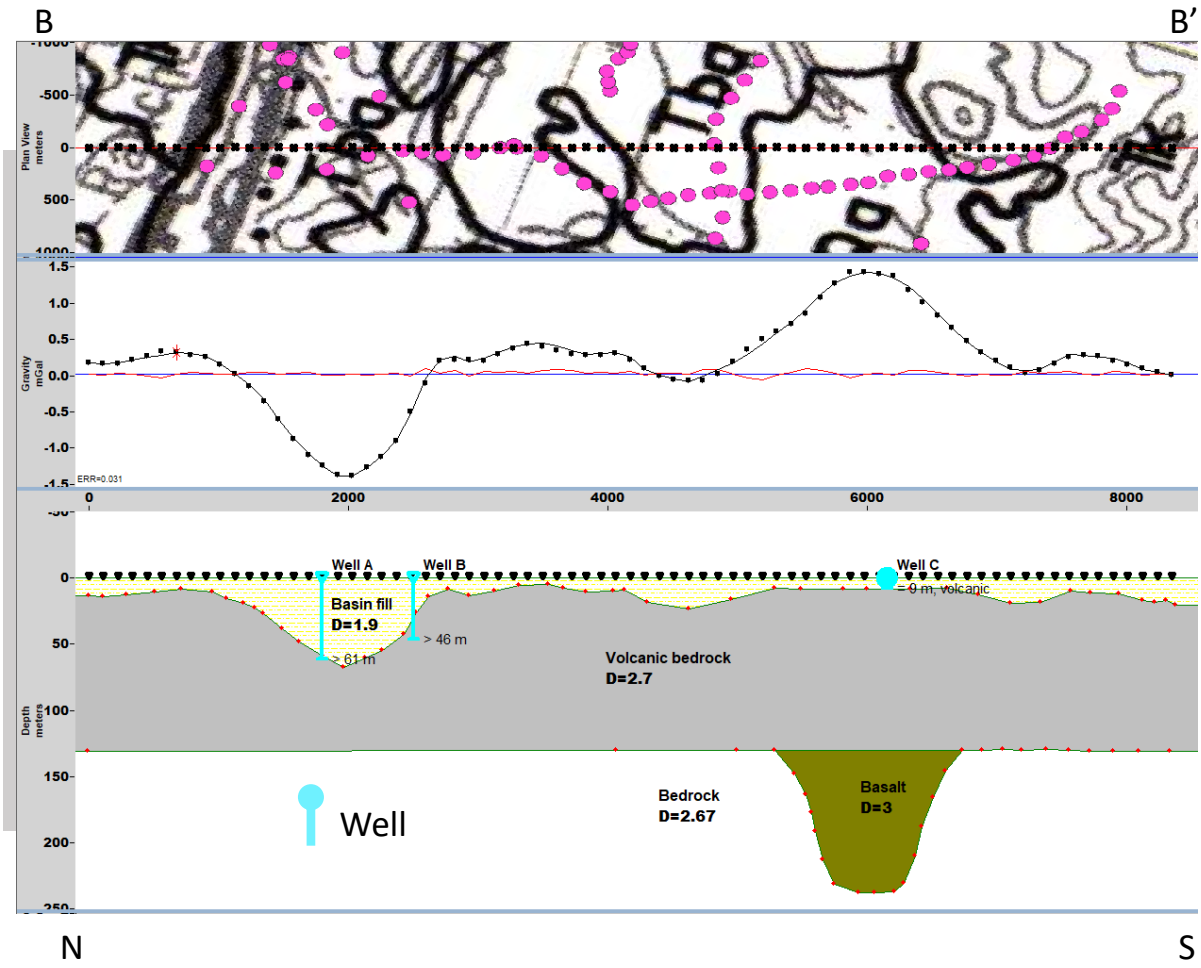

Figure 25. Gravity model for line B-B'. Top panel is a geologic strip map from Figure 20. Middle panel shows gravity data (black circles), gravity model (black line), and residual (red line). Bottom panel shows preferred 2d density model, including control on thickness of Quaternary basin from three wells (light blue line). Dense unit in the south interpreted as a paleochannel filled with denser material than the surrounding igneous bedrock. This could be one of the Oligo-Miocene paleochannels filled with welded tuffs that have been documented at the surface and in the subsurface throughout western Nevada (e.g., Faulds et al., 2005; Henry 2008; Henry and Faulds, 2010; Henry and John, 2013; Sturmer and Faulds, 2018). Map from Greene et al. (1991).

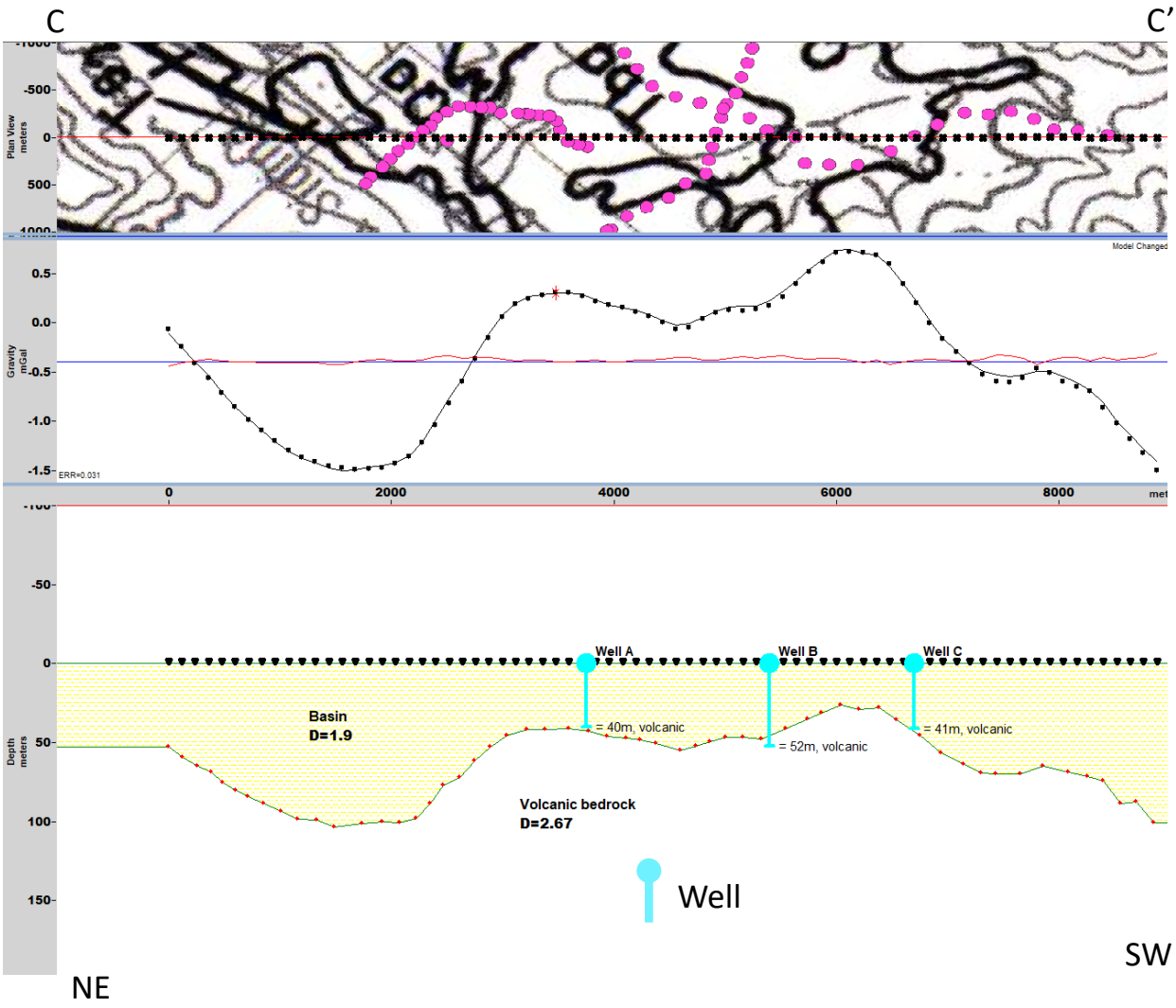

Figure 26. Gravity model for line C-C'. Top panel is a geologic strip map from Figure 20. Middle panel shows gravity data (black circles), gravity model (black line), and residual (red line). Bottom panel shows preferred 2d density model, including control on thickness of Quaternary basin from three wells (light blue lines). Map from Greene et al. (1991).

The 25 well-logs incorporated into the depth to basement map (Figure 27) range in depth to basement (generally defined as basalt or "hard-rock" on the lithology logs). Most of the depths to basement are relatively shallow (0-40 m)The map is defined by both depth to basement within the outline of TRIC basin and by 0-depth points along the outline of the basin. The basin map can be divided into northern and southern portions. The northern portion is along the Interstate 80/Truckee River Corridor. The TRIC basin has two relatively deep centers along a NNE trend, with the deepest values >200 m in the northeastern-most part of the basin. The southern sub-basin is dominated by depths <50 m with the exception of one well log in the southeast, which hits "broken rock" at 128 m depth, generating a small and very deep basin.

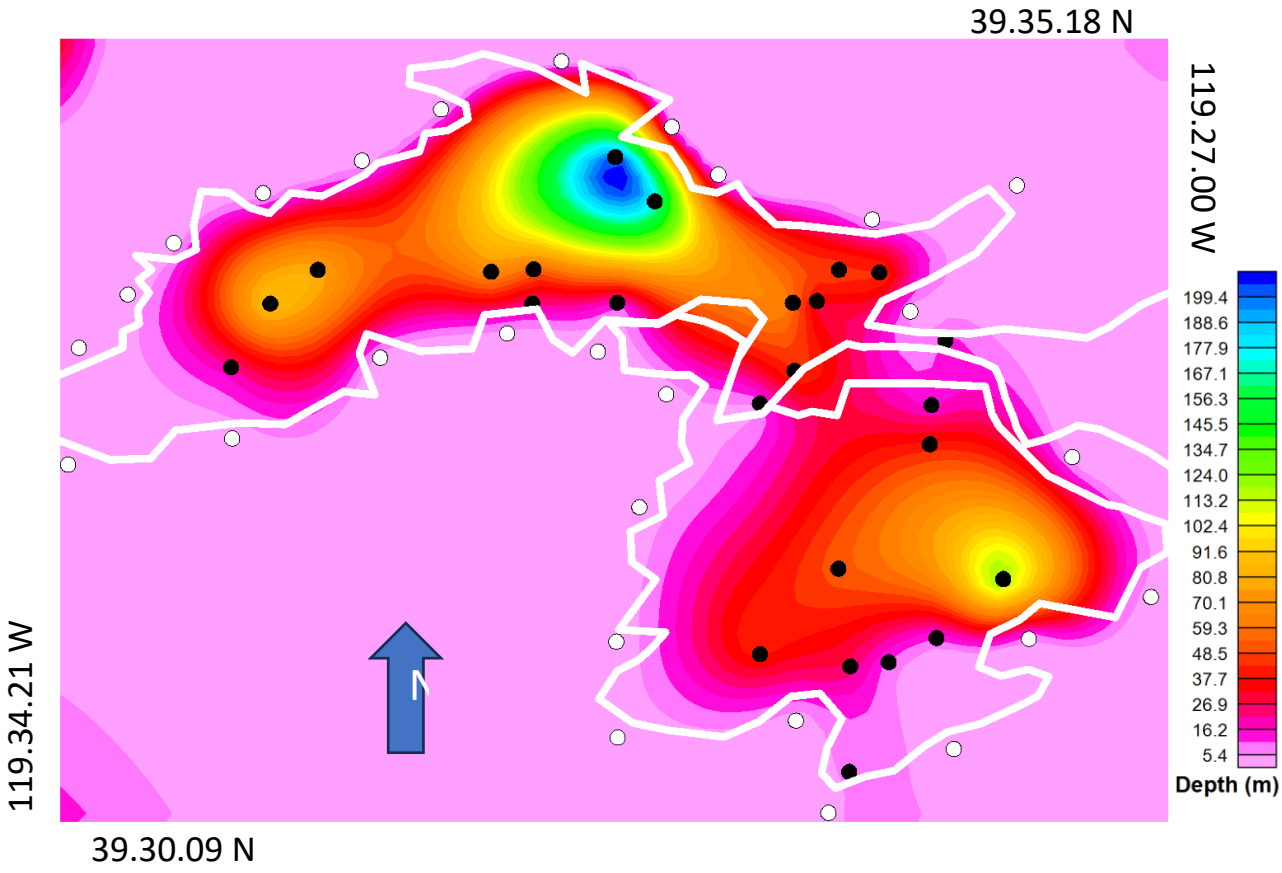

Figure 27. Depth to basement map for the TRIC area based on well log depths to basement. Wells are denoted by black circles. White outline shows approximate basin outline for the TRIC area.

Seismic techniques

In TRIC we deployed four lines of seismic nodes, including two long and two short lines. The long lines include a NNW-trending line along USA Parkway from the southern end of the basin to I-80 (Line 1) and a ENE-trending line across the south-central part of the basin (Line 2). The two shorter lines include a zig-zag line along the Truckee River corridor in the western part of the basin and a NNE-trending line in the east. Note that as much of the area has been sectioned off for factories and industrial development, access across much of TRIC was limited, especially in the northern and eastern parts of the basin. Unfortunately, the deepest part of the basin is likely north of I-80, where we were unable to gain access.

In the ReMi analysis we ran into similar issues with shallow basin depths that we saw on portions of lines 7 and 8 in Lemmon Valley. For these lines, the spacing between individual nodes is so large that a thin depth to basement (< 50 m) is so far unresolvable. However, the HVSR analysis was generally successful for each line.

Line along USA Parkway (Line 1)

Line 1 had 39 nodes deployed across 6.5 km (north-south) with an average spacing of 171 m (Figure 20). Nodes were deployed on Sept. 9, 2023 and they recorded noise for 12 hours, resulting in 24 30-minute records for analysis. Several additional nodes were added toward the end of the data recording for a total of 45 nodes with an average spacing of 147 m. This larger array recorded data for 2 hours. The shallow depth to basement along line 1 and the wide nodal spacing resulted in ReMi analysis not being able to resolve Quaternary basin properties, as the basin thickness was below ReMi vertical resolution.

The HVSR analysis of line 1 (Figure 28) produced a variety of basin depths, mostly focused between 20 and 50 m, with the exception of the central part of the line, with a few depths of 80-110 m (Figure 29). The southern end of the HVSR analysis shows gently increasing depths for ~2 km from 25 to 40 m, followed by a steep increase, with depth values of 50-110 m. The northern 2 km of line 1 show the basin shallowing and flattening out at a depth of 20-25 m. The overall pattern of the basin profile is similar to that derived from the well logs, though that profile shows a clear basinal depression between 2 and 5 km north of the southern end of the line.

ENE-trending line in center of TRIC (Line 2)

Line 2 had 49 nodes deployed across 3.4 km (east-west) with an average spacing of 71 m. Nodes were deployed on Sept. 16, 2023 and they recorded noise for 15 hours, resulting in 30 30-minute records for analysis. As with line 1, the shallow depth to basement and wide nodal spacing resulted in ReMi analysis not being able to resolve Quaternary basin properties, as the basin thickness was below ReMi vertical resolution. The line 2 HVSR analysis shows a generally flat basin floor at ~55 m depth, with a decrease at the eastern end to ~35 m (Figures 30 and 31). This profile contrasts sharply with the model from well logs, which shows an increase from no basin in the west to a plateau at ~30 m depth 1-2 km from the western end, and a rapid deepening to over 200 m. The deep portion is required by one well in the southeastern part of TRIC, through the actual depth to basement in that well is unclear and may be much shallower than the value used here.

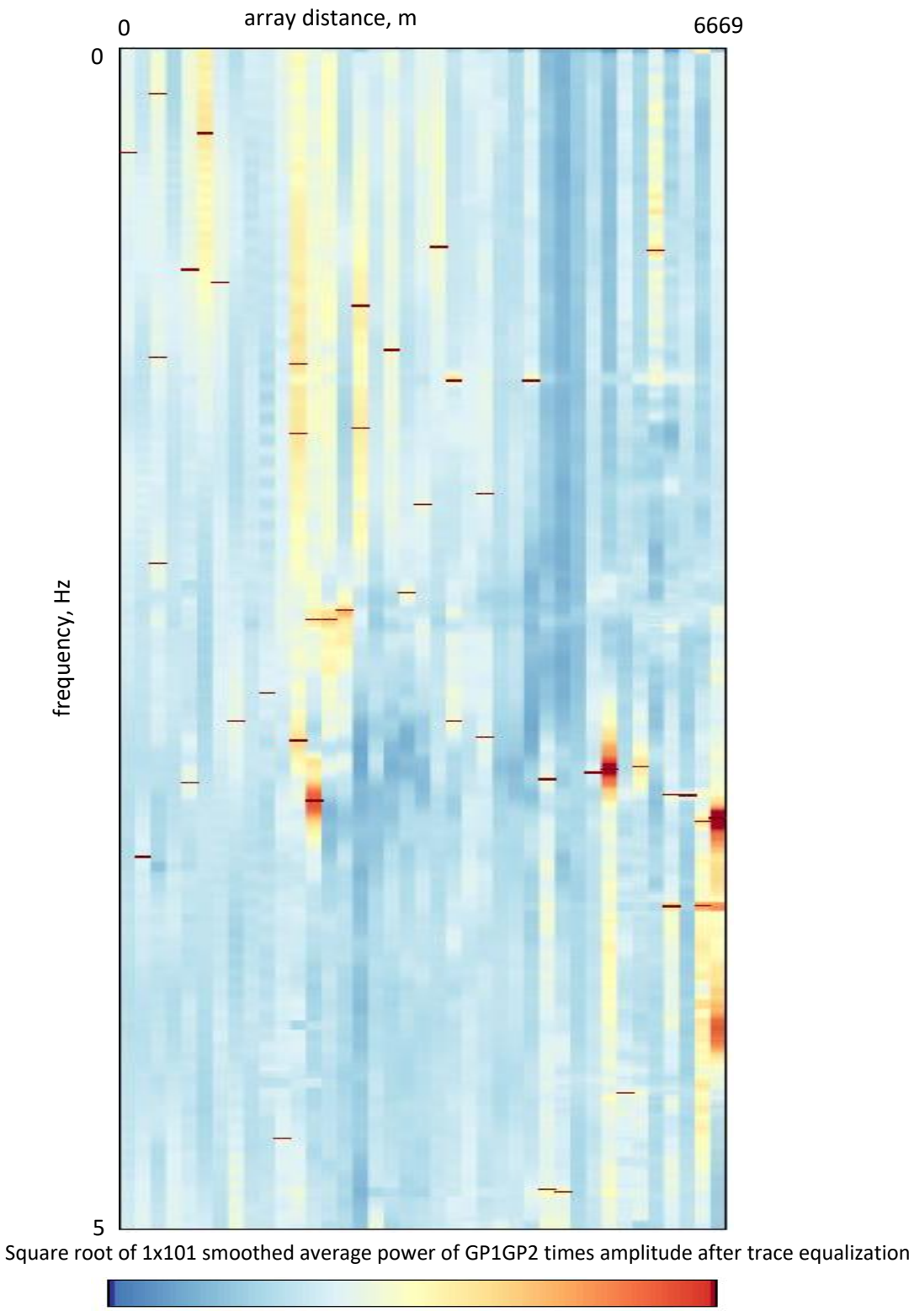

Figure 28. Line 1 HVSR analysis, plotting increasing frequency (y-axis) versus distance along the array (y-axis). Picks for peak power along the line are shown by the red bars.

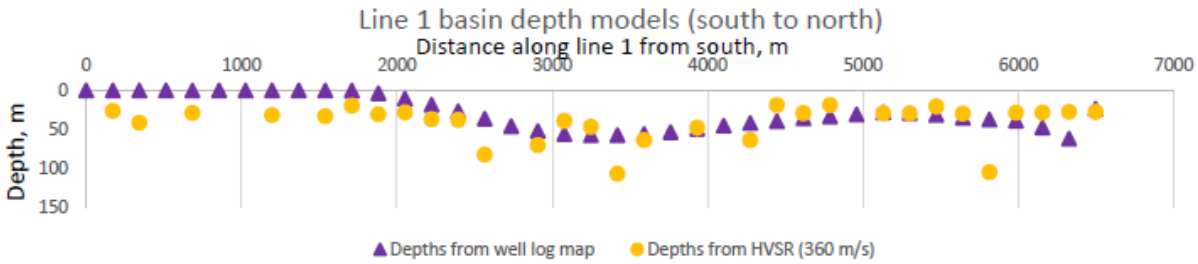

Figure 29. Comparison of depth to basement derived from well log map (triangles) and HVSR (circles) analysis for line 1 along USA Parkway in TRIC. Plotted south (left) to north (right) and scaled at 5x vertical exaggeration.

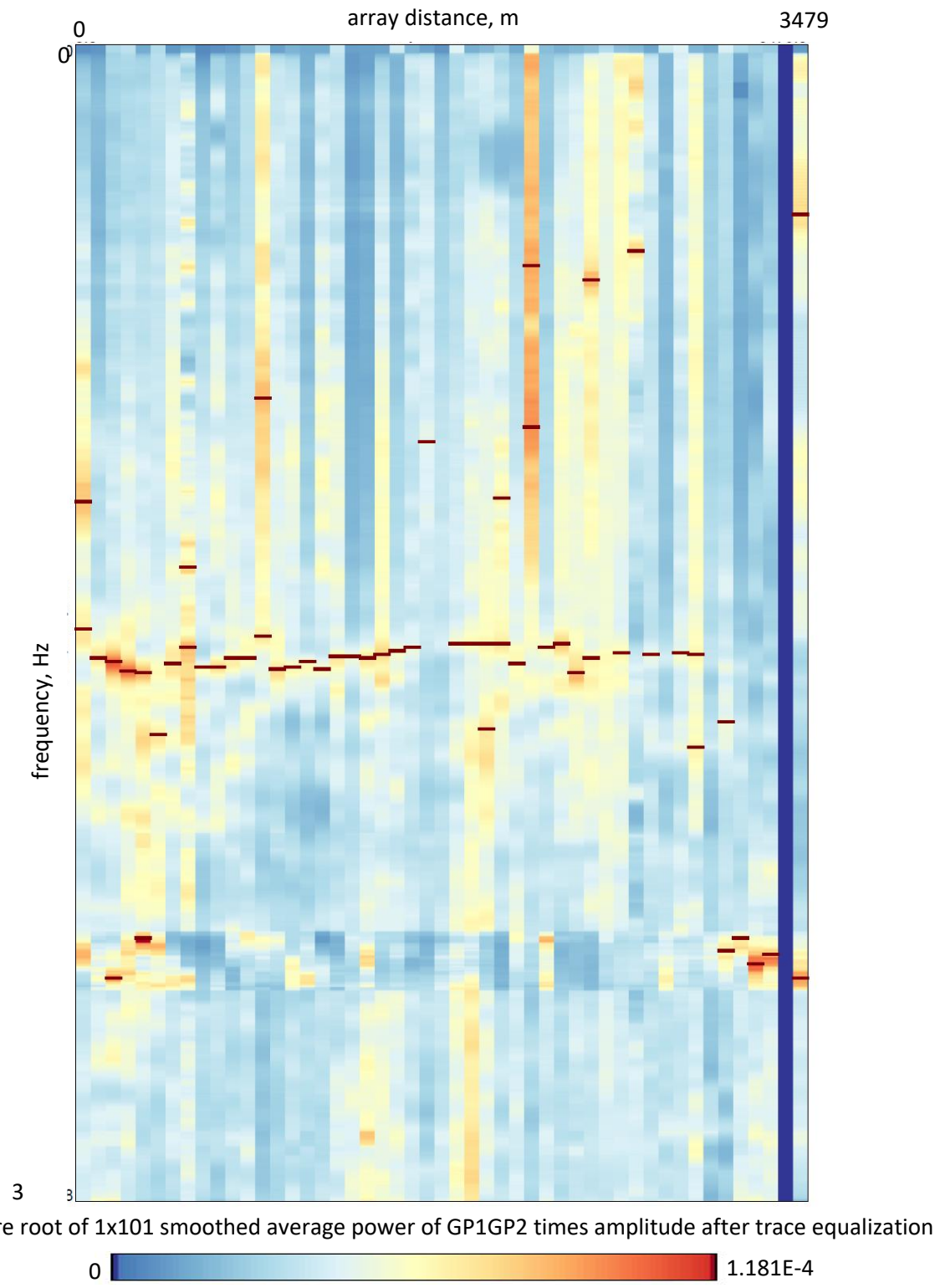

Figure 30. Line 2 HVSR analysis, plotting increasing frequency (y-axis) versus distance along the array (y-axis). Picks for peak power along the line are shown by the red bars.

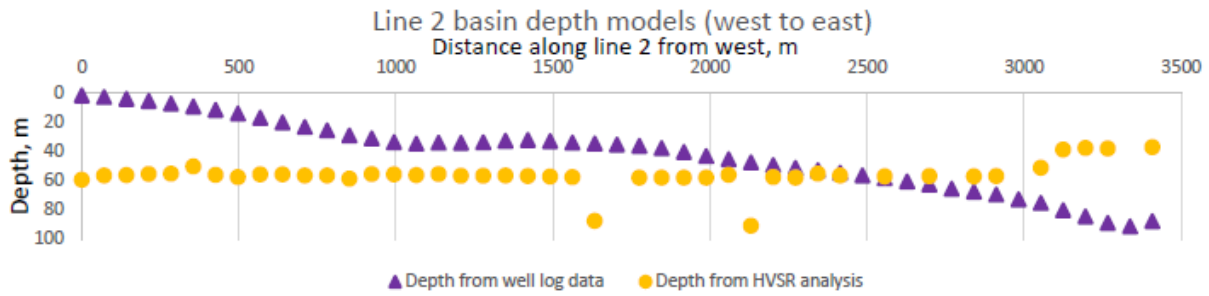

Figure 31. Comparison of depth to basement derived from well log map (triangles) and HVSR (circles) analysis for line 2 in TRIC. Plotted west (left) to east (right) and scaled at 5x vertical exaggeration.

Line along Truckee River (Line 3)

Line 3 had 48 nodes deployed across 2.6 km (east-west) with an average spacing of 54 m. Nodes were deployed on Oct. 8, 2023 and they recorded noise for 3 hours, resulting in 6 30-minute records for analysis. As with lines 1 and 2, the shallow depth to basement and relatively wide nodal spacing resulted in ReMi analysis not being able to resolve Quaternary basin properties, as the basin thickness was below ReMi vertical resolution. The line 3 HVSR results mirror the results from the well log map more than any of the other TRIC lines. Two sets of HVSR data were included, one with the frequency trimmed to 3 Hz (Figure 32), and one that extended frequency to 5 Hz (Figure 33). The 5 Hz data set allowed for more parts of the profile to be picked and generally are in better agreement with the well log basement depths. From the west, the basin increases in thickness from ~10 m to 50-60 m at 1 km from the western end (Figure 34). The basement depths then decrease to ~30 m across the next 1 km of line length. In the final ~0.5 km of line length the depth to basement values vary between 60 and 150 m, which is deeper than the ~20 m from the well-log-derived map.

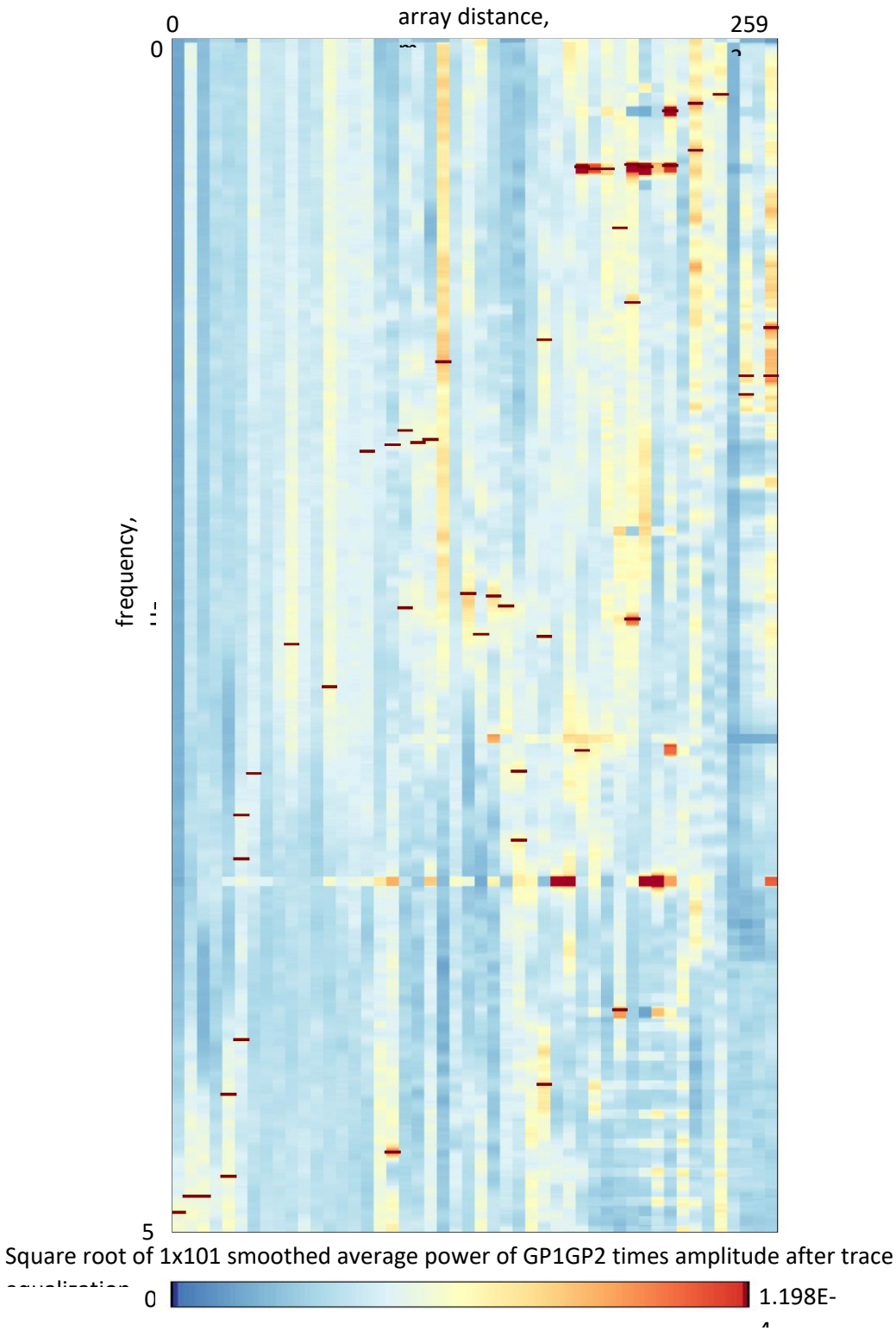

Figure 32. Line 3 HVSR analysis, plotting increasing frequency (y-axis) versus distance along the array (y-axis). This analysis is down to 5 Hz. Picks for peak power along the line are shown by the red bars.

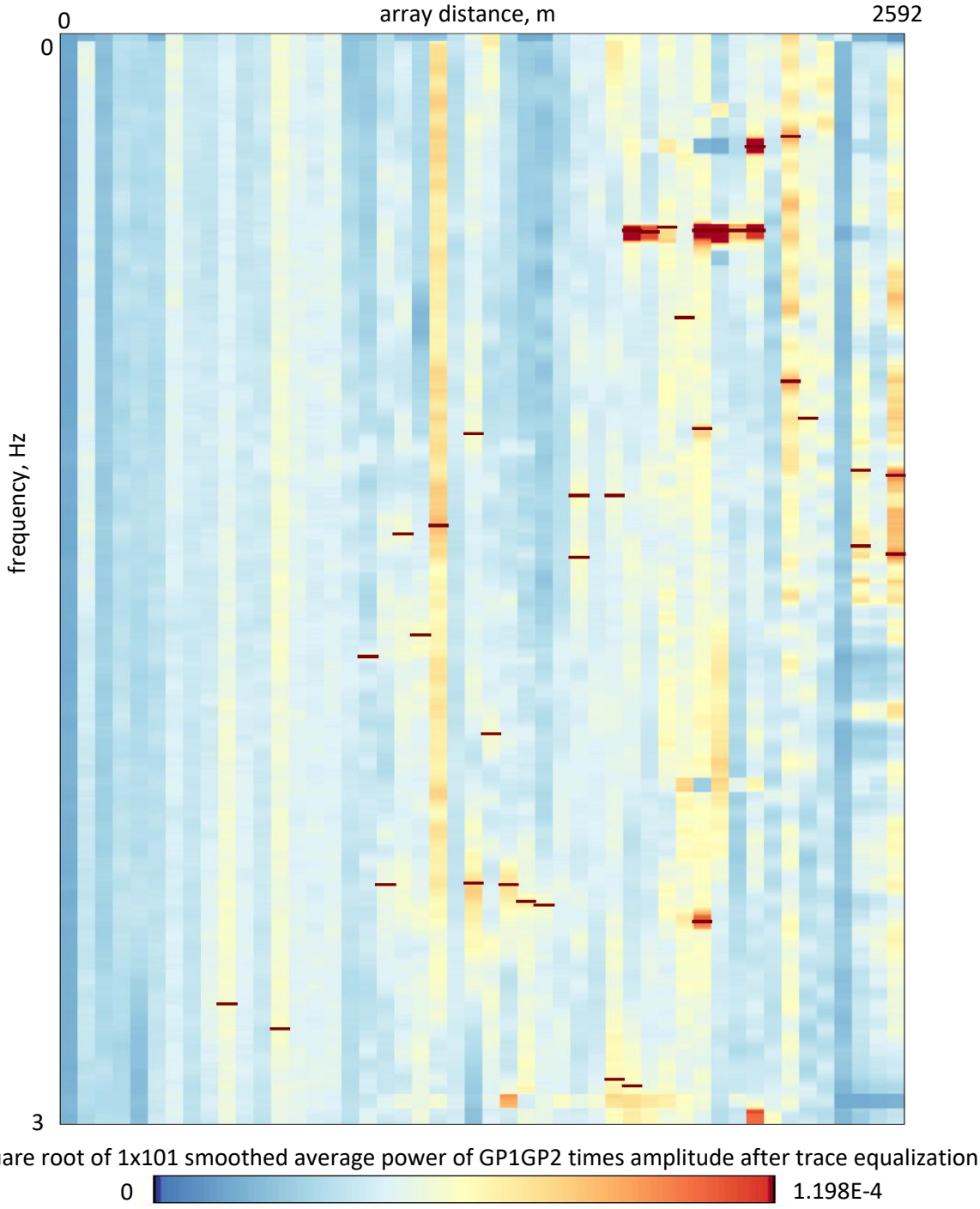

Figure 33. Line 3 HVSR analysis, plotting increasing frequency (y-axis) versus distance along the array (y-axis). This analysis is down to 3 Hz. Picks for peak power along the line are shown by the red bars.

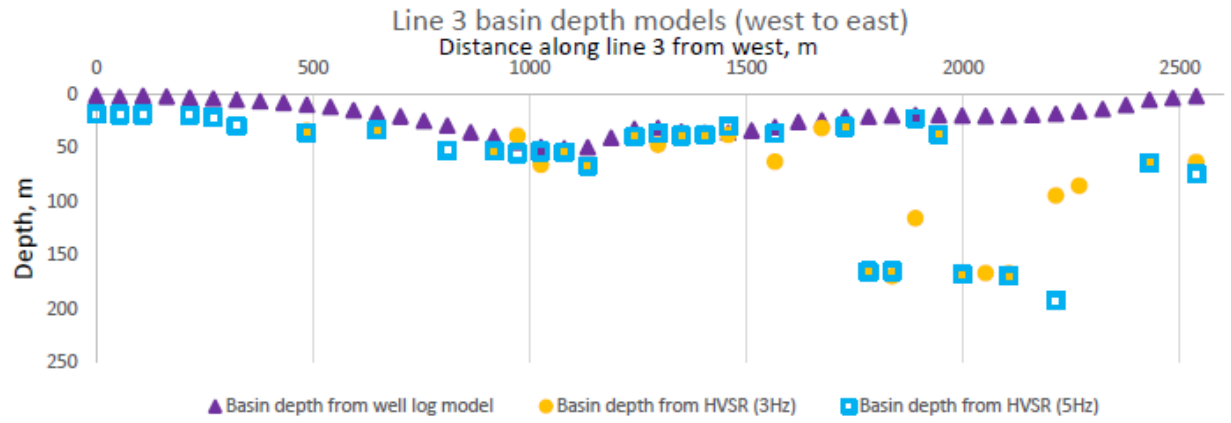

Figure 34. Comparison of depth to basement derived from well log map (triangles) and HVSR analysis at 3 Hz (circles) and 5 Hz (open squares) for line 3 in TRIC. Plotted west (left) to east (right) and scaled at 5x vertical exaggeration.

Line in northeastern TRIC (Line 5)

Line 5 had 39 nodes deployed across 1.1 km (north-south) with an average spacing of 30 m. Nodes were deployed on Oct. 7, 2023 and they recorded noise for 2.5 hours, resulting in 5 30-minute records for analysis. Dispersion curves are quite clear from 3-7 Hz (Figure 35), but the full 2D section could not be completed for this report. The whole-array ReMi analysis shows a Vs30 for the section of 438 m/s with the depth to Vs of 1.0 km/s (Z1.0) at 33 m and the depth to Vs of 2.5 km/s (Z2.5) of 165 m. The Z1.0 value closely matches the depth to basement value derived from HVSR.

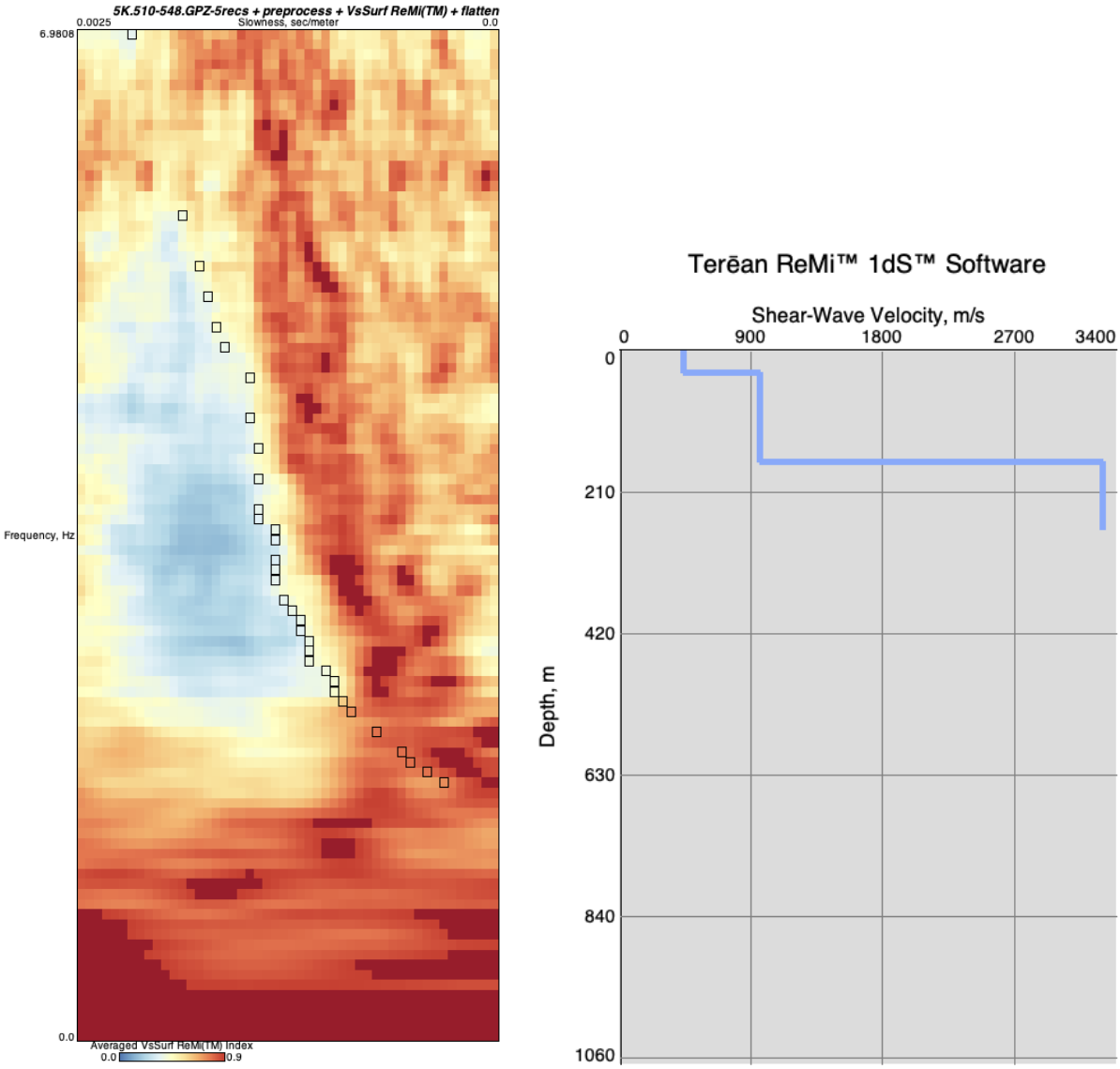

Figure 35. (left) Fundamental-mode Rayleigh-wave dispersion analysis of the Line 5 whole array in the Terean ReMi 1dS™ software. Black squares are dispersion picks. (right) Shear-wave velocity profile for the whole-array Line 5 analysis using Terean ReMi 1dS™ software. The modeled profile reveals a Vs30 of 438 m/s, a Z1.0 of 33 m, and a Z2.5 of 165 m.

The line 5 HVSR analysis shows a relatively flat basin with a depth of 40 m that deepens to 55-70 m toward the north (Figures 36 and 37). This is different than the well log profile that shows the basin first deepening to 100 m, then shallowing to 20 m toward the north. The discrepancy may be in part due to this line being so short. One well depth and the edge of the basin are guiding the well-log-derived profile, whereas the HVSR analysis 33 data points with that same area.

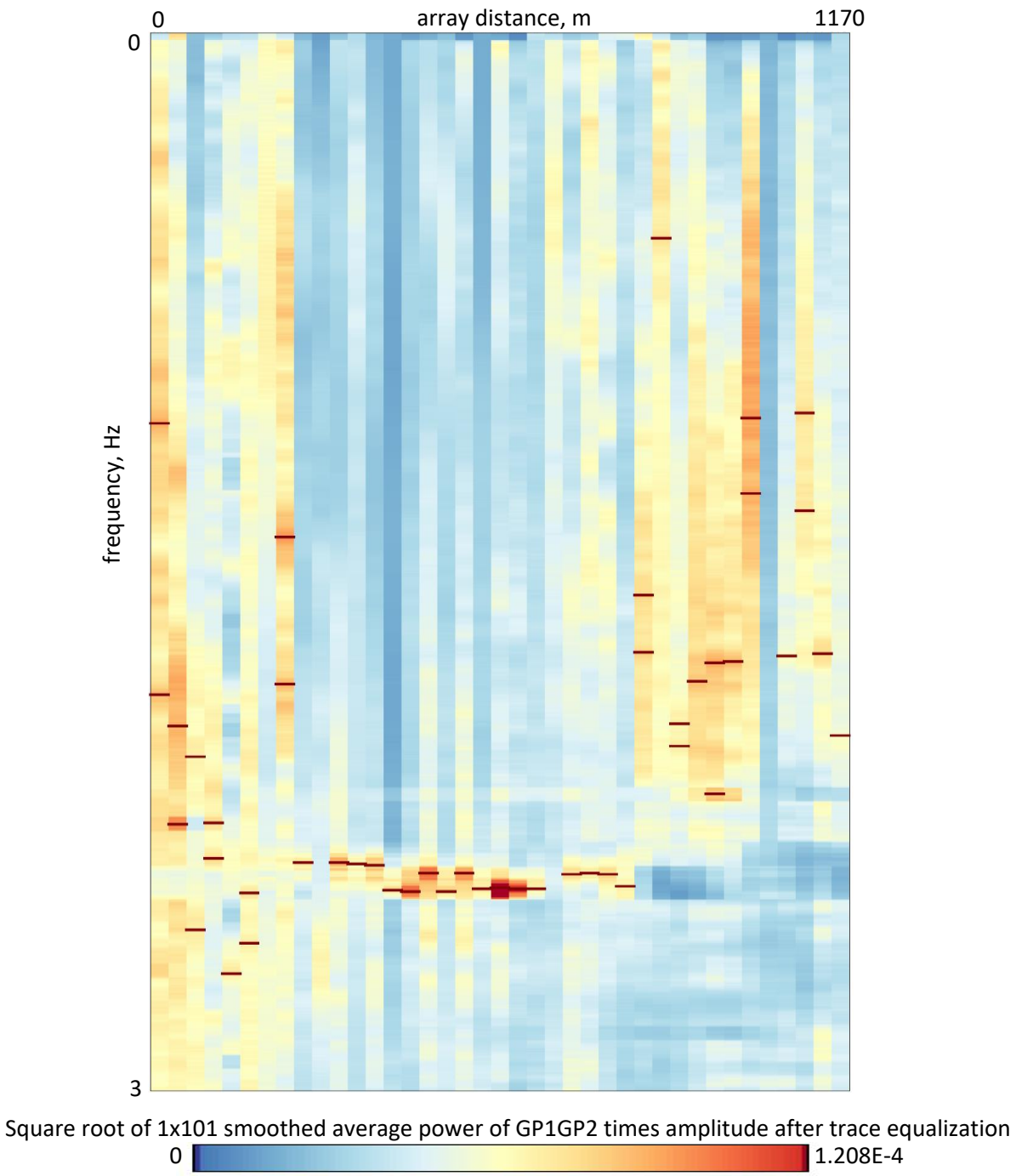

Figure 36. Line 5 HVSR analysis, plotting increasing frequency (y-axis) versus distance along the array (y-axis). Picks for peak power along the line are shown by the red bars.

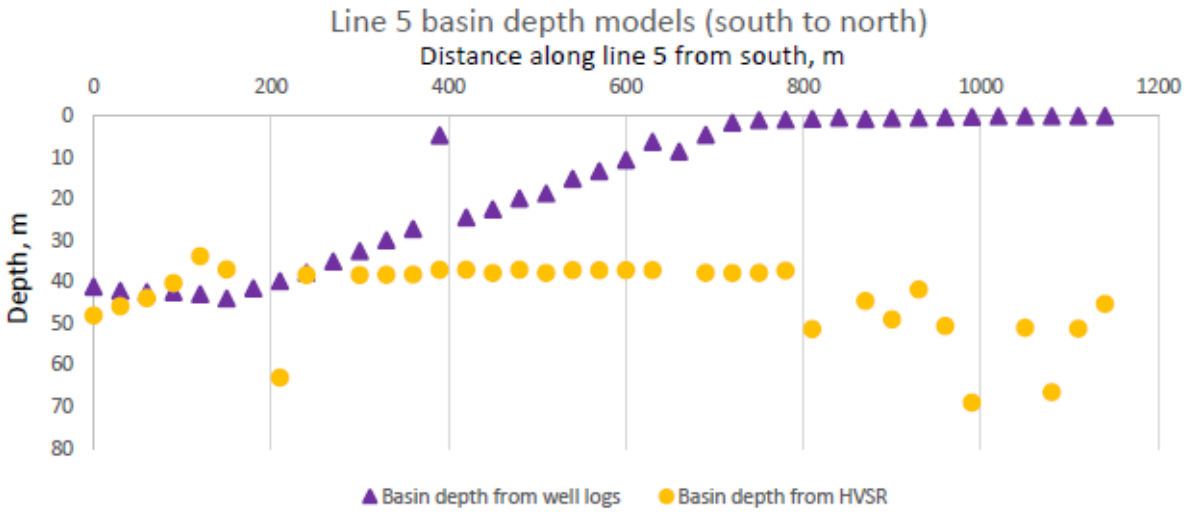

Figure 37. Comparison of depth to basement derived from well log map (triangles) and HVSR (circles) analysis for line 5 in TRIC. Plotted south (left) to north (right) and scaled at 5x vertical exaggeration.

Discussion

Lemmon Valley

The gravity and seismic data demonstrate that Lemmon Valley is an elongate and narrow N-S basin. In E-W profiles, the basin is fairly symmetric, consistent with normal faults being present on both sides of the basin (e.g., Soeller and Nielsen, 1980). Basin depth increases southward, reaching a maximum of ~850 m below Silver Lake. Z1.0 values also generally increase in depth southward across the basin from near the surface in the north to ~300 m depth around Silver Lake and increasing to 200 m depth at the southern end of the basin. The variety of basin depth and basin shape suggest that the area would experience a wide variety in the acceleration and shaking duration during a given earthquake.

TRIC

In contrast to Lemmon Valley, the TRIC basin is generally very shallow (less than ~50 m) except in the northern park of the basin. Even the northern part of the basin is only a few hundred m deep. The gravity-derived depths in TRIC represent Z1.0, the depth to a shear-wave velocity of 1.0 km/s, instead of Z2.5, the depth to a shear-wave velocity of 2.5 km/s. The shallow volcanic rocks at TRIC, which gravity sees as local basement, tend to have shear-wave velocities above 1.0 km/s but still below 2.5 km/s (Pancha et al., 2017; Simpson and Louie, 2020). The Saltus and Jachens (1995), Abbott and Louie (2000), and this project's gravity depths in Lemmon Valley all represent Z2.5. Overall the deeper parts of the basin are much smaller than the basins around Lemmon Valley. This is likely because the basins in the northern part of TRIC are small pull-apart basins that formed between left-stepping strands of the Olinghouse fault at and north of the Truckee River (e.g., Sturmer, 2007; Sturmer and Faulds, 2018). The combination of more complex volcanic stratigraphy and poor access made the analysis of TRIC

much more complex than that of Lemmon Valley. However, even with those challenges, it appears there will be less variability in acceleration and shaking duration across the TRIC area than in the Lemmon Valley area.

Improvements to CVM

The resolution in the CVM was significantly improved with addition of the results from this study. Prior to this study, the Lemmon Valley area had a relatively flat depth to basement with an average value of ~100 m depth (Figure 38). The addition of this work captures the deep and narrow north-trending Lemmon Valley, in addition to new detail in White Lake Valley, Golden Valley, and Hungry Valley (Figure 39). In TRIC, previously there was a large area of greater than 1 km depth centered around the TRIC and Pyramid sequence area from Saltus and Jachens (1995), representing the estimated depth to Mesozoic basement below the thick volcanic sequence. Our work shows that the depth of the Quaternary sedimentary basin above Tertiary volcanics is much shallower throughout TRIC, though complexities between the Miocene volcanic section and Mesozoic basement still deserve more attention. Overall, this work has allowed for much finer resolution within the CVM which will allow workers to better evaluate shaking hazard in these important industrial areas for a variety of earthquake sources. This in turn, will help us to determine the types of protection that will be needed to prevent structural failure (and associated loss of life) during a large earthquake in the area.

Conclusions

1. Measuring closely spaced gravity lines in the Lemmon Valley area, adding to a background of moderately spaced prior measurements, quickly and effectively allowed detailed characterization of basement depth, representing Z2.5. The TRIC has only very sparse pre-existing gravity measurements, so well-log info proved more effective than gravity lines at constructing a Tertiary-basement depth map, representing Z1.0.
2. Long lines of widely spaced 3-component nodal seismic recorders proved effective at recovering shear-wave velocity versus depth cross sections using passive-source ReMi analysis, where basin thickness was greater than recorder spacing. Lines 5, 9, and the western portion of Line 7 met this condition. Along these lines, ReMi analysis recovered basin velocity profiles, basement velocities, Z1.0, and Z2.5.
3. Using the HVSR technique, most 3-component stations yielded microtremor spectral-ratio peak frequencies. Where shear-wave velocities were also available, at Lines 5, 7, and 9, the HVSR frequencies suggested depths in agreement with Z1.0 and Z2.5. Velocities had to be assumed for HVSR analysis of other lines.
4. Combining the gravity and seismic information with rock depths from well logs produced a detailed Z2.5 map of Lemmon Valley for addition to the Reno-area CVM, at a lateral resolution of 200 m.
5. Well-log rock depths at the TRIC are in general agreement with approximate depths derived from ReMi, HVSR, and gravity analyses. The TRIC addition to the Reno-area CVM is a map of Z1.0 at 200 m lateral resolution.

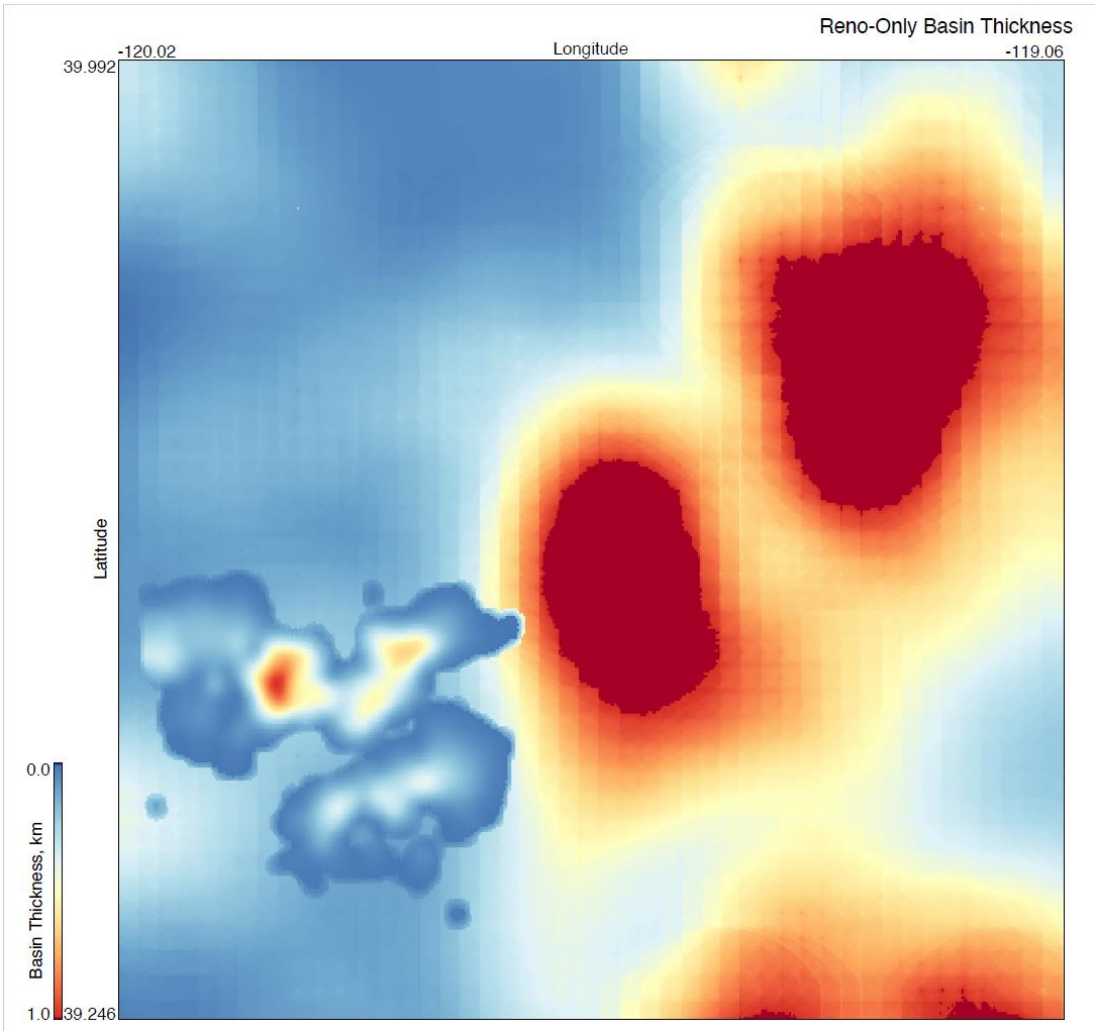

Figure 38. Basin thickness from CVM before this study. Detailed area is for the Reno-area basin.

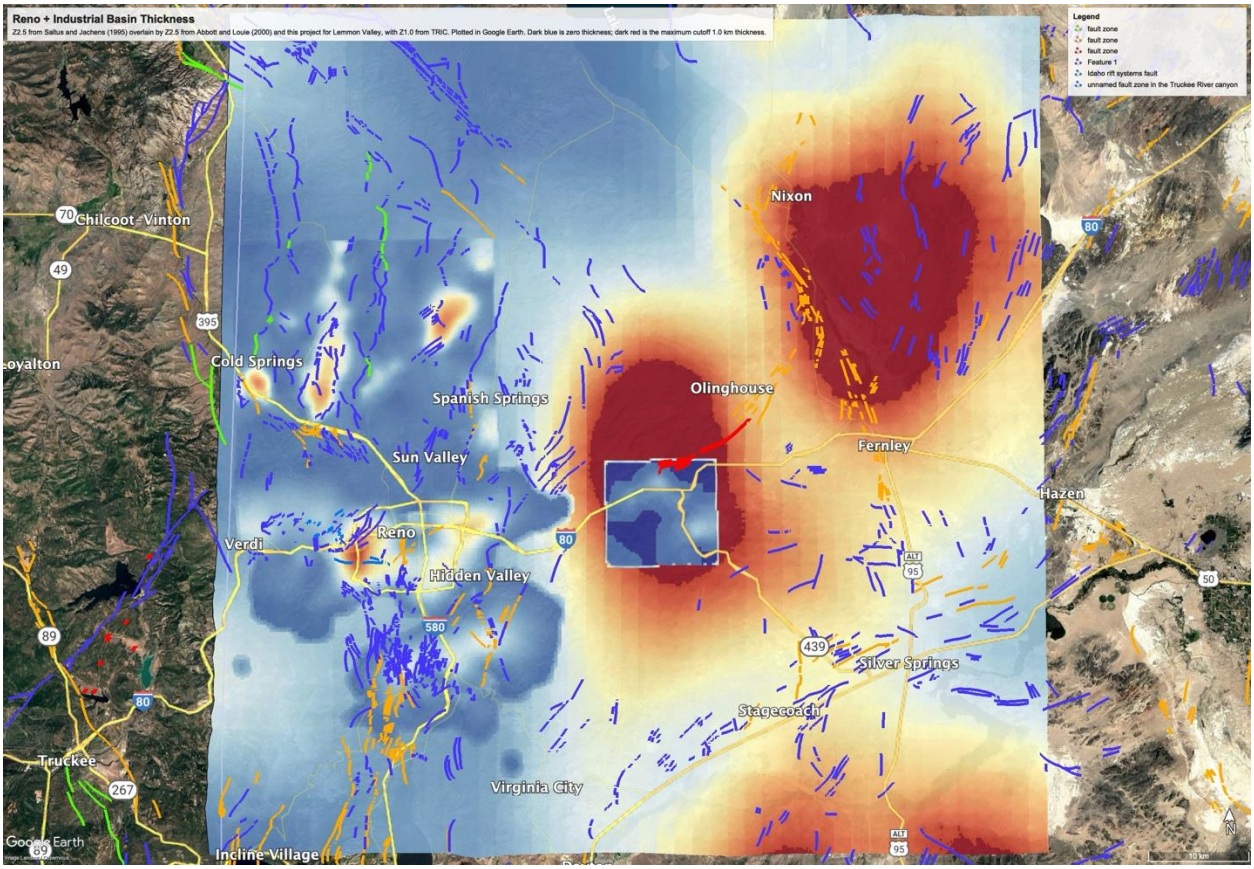

Figure 39. Z2.5 from Saltus and Jachens (1995) overlain by Z2.5 from Abbott and Louie (2000) and this project for Lemmon Valley, with Z1.0 from TRIC. Plotted in Google Earth. Dark blue is zero thickness; dark red is the maximum cutoff 1.0 km thickness.

Future work

In the process of preparing journal articles resulting from this project over the next year, the project team will conduct the following further analyses:

1. Complete the development of the Line 5 2D shear-wave velocity cross section in the Terēan ReMi 2dS™ software.
2. Further explore the surface-wave dispersion-curve results that can be obtained by non-interferometric as well as interferometric surface-wave analysis for the lines that did not easily yield ReMi results: Line 1, Line 2, Line 3, the eastern end of Line 7, and Line 8. These lines had a seismic sensor spacing wider than their basin thicknesses.
3. UNR-CTEMPs and Terēan will continue to conduct standard geotechnical ReMi surveys for Vs30 along all lines, and bring those results into the public ReMi Vs30 database. As well, Terēan will gather geotechnical ReMi survey results in the region contributed to the public by Terēan clients, adding those to the database as well.

Further research employing this project's results will be proposed, possibly encompassing the following tasks on the 3-5 year time frame:

1. In the TRIC area a stronger background of gravity measurements needs to be established, extending into the areas of Mesozoic basement to the east. An ideal grid spacing for this gravity network would be about 0.5 km. This background network must be established in close collaboration with Storey County, the Nevada Department of Transportation, and the many large landowners and developers in the TRIC region.
2. The Nevada ShakeZoning 3D model assembler needs re-working to accomplish the following technical goals:
    a. Allowing the detailed deep-basin velocity profiles developed by this project and by Pancha et al. (2017) for the Reno region to affect the lateral shear-wave-velocity heterogeneity of the basin fill as well as the top of the basement, to 1.5 km depth.
    b. Allow the input of Z1.0 as well as Z2.5 surfaces in the development of CVMs, using all data where available. This improvement will avoid the artificial jumps in basin thickness where Z1.0-only models are near Z2.5-only models.
3. After completing the fully laterally variable CVM for Reno and its industrial areas, run a large number of physics-based deterministic shaking scenario computations for frequencies up to 3 Hz (in the manner of Eckert et al., 2021), for a non-ergodic view of shaking intensity and duration, and basin amplification. These runs will include validation of computed shaking spectra against shaking spectra of recorded earthquakes.

Acknowledgments

We thank the USGS and NEHRP program for giving us funding to compete this work. This material is based upon work supported by the U.S. Geological Survey under Grant Numbers G23AP00242 and G23AP00244. The views and conclusions contained in this document are those of the authors and should not be interpreted as representing the opinions or policies of the U.S. Geological Survey. Mention of trade names or commercial products does not constitute their endorsement by the U.S. Geological Survey. We also thank CTEMPs for allowing use of their gravity equipment. This material is based on services provided by the NSF GAGE Facility at New Mexico Tech, operated by the EarthScope Consortium, with support from the National Science Foundation, the National Aeronautics and Space Administration, and the U.S. Geological Survey under NSF Cooperative Agreement EAR-1724794. Finally, we thank Terēan for use of the software that made the seismic analyses possible.

Data availability

All seismic data related to this study are available on the IRIS website (https://ds.iris.edu/gmap/#network=5K&datacenter=IRISPH5&planet=earth), with all of the data part of survey 5K. Gravity data, both gravity and seismic analysis products, and the CVM products are all housed on PI Louie's website: https://sites.google.com/view/nevada-shake-zoning.

Publications and Presentations Partially Supported by this grant.

Meeting abstracts

Louie, J.N., Lewright, L., Newton, M.O., Pancha, A., and Stern, T., 2024, Exploring basin amplification within the Reno, Nevada and Wellington, New Zealand metropolitan areas with non-ergodic physics-based 3D scenarios: presented at the *Earthquake Engineering Research Institute 2024 Annual Meeting*, Seattle, WA, 10 April. Available at https://drive.google.com/open?id=16ygJ2HPIa-MO6eomN_n2jYThF_7rW5il&usp=drive_fs

Louie, J., 2024, Simplified seismic surveys for non-intrusive ASCE 7-22 compliant site class, rippability, fault location, and design: presented at *Association of Environmental and Engineering Geologists 2024 Annual Meeting*, Philadelphia, PA, 12 September. Available at https://drive.google.com/open?id=1GPDkl_iV9NZmvtziC7plje4RjXCNd-sL&usp=drive_fs

Smith, P., Kratt, C.B., **Sturmer, D.,** Gautschi, O., Meharwal, E., Sayyadi, S., Castle, G., and Louie, J., 2024, 2.5-D gravity models from Lemmon Valley and the Tahoe-Reno Industrial Center, western Nevada, USA: accepted for poster presentation at 2024 AGU national meeting.

Smith, P., Kratt, C., Louie, J.N., **Sturmer, D.,** and Gautschi, O., 2024, Preliminary 2.5-D gravity models from Lemmon Valley and the Tahoe-Reno Industrial Center, western Nevada: poster presentation at the 2024 joint Cordilleran-Rocky Mountain GSA section meeting.

Sturmer, D., and Louie, J.N., 2024, Evaluating recent tectonic evolution of two Reno-area basins through deep refraction-microtremor analysis, western NV: poster presentation at the 2024 joint Cordilleran-Rocky Mountain GSA section meeting.

Theses

Smith, P., 2024, Gravitational mapping of subsurface rock to aid earthquake risk assessment [B.S. thesis]: Cincinnati, Ohio; Department of Physics, University of Cincinnati, 41 p.

References Cited

Abbott, R.E., Louie, J.N., 2000, Depth to bedrock using gravimetry in the Reno and Carson City, Nevada area basins. Geophysics 65, 340-350.

Bonnefoy-Claudet, S., Cornou, C., Bard, P.-Y., Cotton, F., Moczo, P., Kristek, J., and Fäh, D., 2006, HVSR ratio: a tool for site effects evaluation: *Geophysical Journal International*, **167**, 827-837.

Briggs, R.W., Wesnousky, S.G., 2005. Late Pleistocene and Holocene paleoearthquake activity of the Olinghouse fault zone, Nevada. Bull. Seismol. Soc. Am. 95, 1301–1313. 10.1785/0120040129.

Cashman, P.H., Fontaine, S.A., 2000. Strain partitioning in the northern Walker Lane, western Nevada and northeastern California. Tectonophysics 326, 111–130.

Cashman, P.H., Trexler, J.H., Jr., Widmer, M.C., and Queen, S.J., 2012: Post-2.6 Ma tectonic and topographic evolution of the northeastern Sierra Nevada: The record in the Reno and Verdi basins. Geosphere, vol. 8, no. 5.

Cordy, G.E. and Mansour, A., 1985, Reno NE Quadrangle geologic map: Nevada Bureau of Mines and Geology Urban Map UM4Cg, scale 1:24,000.
Eckert E., M. Scalise, J.N. Louie, and K.D. Smith, 2021, Exploring basin amplification within the Reno metropolitan area in Northern Nevada using a magnitude 6.3 ShakeOut scenario: *Bulletin of the Seismological Society of America*, **112**(1), 457-473, doi: 10.1785/0120200309.
Faulds, J.E., Henry, C.D., 2008. Tectonic influences on the spatial and temporal evolution of the Walker Lane: an incipient transform fault along the evolving Pacific – north American plate boundary. In: Spencer, J.E., Titley, S.R. (Eds.), Circum-Pacific Tectonics, Geologic Evolution, and Ore Deposits. Arizona Geological Society Digest 22, Tucson, Arizona, pp. 437–470.
Faulds, J.E., Ramelli, A.R., Henry, C.D., 2008. Preliminary Geologic Map of the Fernley West Quadrangle, Lyon, Storey, and Washoe Counties, Nevada. Nevada Bureau of Mines and Geology Open-File Report 08-04, scale 1:24,000.
Faulds, J.E., Henry, C.D., Hinz, N.H., 2005, Kinematics of the northern Walker Lane: an incipient transform fault along the Pacific-North American plate boundary. Geology 33, 505–508.
Greene, R.C., Stewart, J.H., John, D.A., Hardyman, R.F., Silberling, N.J., and Sorensen, M.L., 1991, Geologic map of the Reno 1° by 2° quadrangle, Nevada and California: USGS Miscellaneous Field Studies map MF-2154-A, scale 1:250,000.
Hanford, E.J., 2024, Hydrogeology of Golden Valley, Nevada – A Case Study: Report fro Golden Valley Property Owners Association, 227 p., doi: 10.13140/RG.2.2.29925.37603.
Henry, C.D., 2008. Ash-flow tuffs and paleovalleys in northeastern Nevada: implications for Eocene paleogeography and extension in the Sevier hinterland, northern Great Basin. Geosphere 4, 1–35. https://doi.org/10.1130/GES00122.1.
Henry, C.D., Faulds, J.E., 2010. Ash-flow tuffs in the Nine Hill, Nevada, paleovalley and implications for tectonism and volcanism of the western Great Basin, USA. Geosphere, 6, 339–369. https://doi.org/10.1130/GES00548.1.
Henry, C.D., John, D.A., 2013. Magmatism, ash-flow tuffs, and calderas of the ignimbrite flareup in the western Nevada volcanic field, Great Basin, USA. Geosphere 9, 951–1008.
Jachens, R.C., and Moring, B.C, 1990. Maps of thickness of Cenozoic deposits and isostatic resiual gravity over basement in Nevada: U.S. Geological Survey Open-File Report 90-404.
Kelly, T.S., and Secord, R., 2009, Biostratigraphy of the Hunter Creek Sandstone, Verdi Basin, Washoe County, Nevada, *in* Oldow, J.S., and Cashman, P.H., eds., Late Cenozoic Structure and Evolution of the Great Basin–Sierra Nevada Transition: Geological Society of America Special Paper 447, p. 133–146, doi:10.1130/2009.2447(08)
Li, X., Huang, W., Pierce, I.K.D., Angster, S.J., Wesnousky, S.G., 2017. Characterizing the quaternary expression of active faulting along the Olinghouse, Carson, and Wabuska lineaments of the walker Lane. Geosphere 13. https://doi.org/10.1130/GES01483.1.
Louie, J.N., 2001, Faster, better: Shear-wave velocity to 100 meters depth from refraction microtremor arrays, *Bulletin of the Seismological Society of America*, **91**, 347-364.
Louie, J.N., 2020, *ReMi Vs(z) Profile Archive (Version 2.0.0)* [Data set]: doi: 10.5281/zenodo.3951865 .
Louie, J., Pancha, A., and Pullammanappallil, S., 2017, Applications of Refraction Microtremor done right, and pitfalls of microtremor arrays done wrong: 16WCEE Paper 4947, Santiago, 12 pp.

Louie, J.N., Pancha, A., and Kissane,B., 2021, Guidelines and pitfalls of refraction microtremor surveys: *Journal of Seismology*, June 7, doi: 10.1007/s10950-021-10020-5.

Nevada State Rail Plan, 2021, Nevada Dept. of Transportation: 302 pp. Last accessed 22 May 2022, https://www.dot.nv.gov/mobility/rail-planning/state-rail-plan

Pancha, A., and Pullammanappallil, S., 2014, Determination of 3D-velocity structure across the northeastern portion of the Reno area basin, Final Technical Report, External Grant Award No. **G14AP00020**, 27 pp. http://earthquake.usgs.gov/research/external/reports/G14AP00020.pdf.

Pancha, A., Anderson, J.G., Biasi, A., and Anooshepor, A., 2015, An Empirical site response and comparison with measured site conditions at ANSS sites in the vicinity of Reno, Nevada: *Bulletin of the Seismological Society of America*, **105**(2A), 889-911.

Pancha, A., Pullammanappallil, S., Louie, J.N., Cashman, P.H., and Trexler, J.H., Jr., 2017, Determination of 3D basin shear-wave velocity structure using ambient noise in an urban environment: A case study from Reno, Nevada: *Bull. Seis. Soc.Am.*, **107**(6), 3004-3022, doi: 10.1785/0120170136.

Perton, M., Spica, Z.J., Clayton, R.W., and Beroza, G.C., 2020, Shear wave structure of a transect of the Los Angeles basin from multimode surface waves and HVSR spectral ratio analysis, *Geophysical Journal International*, **220**(1), 415-427.

Pullammanappallil, S., 2016, Determination of deep shear-velocity structure across the Reno-area basin:Final Technical Report to the U.S. Geological Survey, External Grant Award No. **G15AP00055**, 31pp. http://earthquake.usgs.gov/research/external/reports/ G15AP00055.pdf

Ramelli, A.R., dePolo, C.M., and Bell, J.W., 2003, Paleoseismic studies of the Peavine Peak fault: Technical report to USGS, Reston, Virginia, under Contract **01HQGR0167**, 14 pp.

Ramelli, A.R., Henry, C.D., Walker, J.P., with contributions by Bell, J.W., Cashman, P.H., dePolo, C.M., Garside, L.J., House, P.K., Trexler, J.H., and Widmer, M.C., 2011, Preliminary revised geologic maps of the Reno urban area, Nevada: Nevada Bureau of Mines and Geology Open-File Report 11-7, 3 plates, scale 1:24,000.

Rose, R.L., 1969, Geologic map and sections of parts of the Wadsworth and Churchill Butte Quadrangles, Nevada: Nevada Bureau of Mines and Geology Bulletin 71, scale 1:48,000.

Saltus, R. W., and Jachens, R. C., 1995, Gravity and basin-depth maps of the Basin and Range Province, Western United States. U.S. Geological Survey, Geoph. Invest. Map, Report: **GP-1012**, 1 sheet.

Schwartz, K.M., 2001. Evolution of the Middle to Late Miocene Chalk Hills Basin in the Basin and Range-Sierra Nevada Transition Zone, Western Nevada. M.S. thesis. University of Nevada, Reno.

Schwartz, K.M., and Faulds, J.E., 2004, Preliminary geologic map of most of the Chalk Hills quadrangle, Storey County, Nevada: Nevada Bureau of Mines and Geology Open-File Report 04-11, scale 1:24,000.

SESAME, 2005, Guidelines for the implementation of the HVSR spectral ratio technique on ambient vibrations - measurements, processing and interpretations: SESAME European research project, deliverable D23.12, accessed 21 May 2021, www.geopsy.org/documentation/geopsy/hv.html.

Simpson, A.R., and Louie, J.N., 2020, Measurements and Predictions of Vs30, Z1.0, and Z2.5 in Nevada (Version 2.0), publ. of the NSL, Zenodo, 28 pp. plus data, maps, doi: 10.5281/zenodo.4408557.

Smith, P., 2024, Gravitational mapping of subsurface rock to aid earthquake risk assessment [B.S. thesis]: Cincinnati, Ohio; Department of Physics, University of Cincinnati, 41 p.
Soeller, S.A., and Nielsen, R.L., 1980, Reno NW Quadrangle geologic map: Nevada Bureau of Mines and Geology Urban Map UM4Dg, scale 1:24,000.
Stewart, J.H., 1988. Tectonics of the Walker Lane belt, western Great Basin: Mesozoic and Cenozoic deformation in a zone of shear. In: Ernst, W.G. (Ed.), Metamorphism and Crustal Evolution of the Western United States (Rubey Volume VII). Prentice Hall, Englewood Cliffs, New Jersey, pp. 683–712.
Sturmer, D.M., 2007, Geometry and kinematics of the Olinghouse fault zone: role of left-lateral faulting in the right-lateral Walker Lane, western Nevada [M.S. thesis]: Reno, University of Nevada, Reno, 117 p.
Sturmer, D.M., and Faulds, J.E., 2018, Kinematic evolution of the Olinghouse fault and the role of a major sinistral fault in the Walker Lane dextral shear zone, Nevada, USA: Journal of Structural Geology, 115, p. 47-63, https://doi.org/10.1016/j.jsg.2018.07.006
Trexler, J., Cashman, P., and Cosca, M., 2012, Constraints on the history and topography of the northeastern Sierra Nevada from a Neogene sedimentary basin in the Reno-Verdi area, western Nevada: Geosphere, v. 8, p. 548-561.
Trexler Jr., J.H., Cashman, P.H., Henry, C.D., Muntean, T., Schwartz, K., TenBrink, A., Faulds, J.E., Perkins, M., Kelly, T., 2000. Neogene basins in western Nevada document the tectonic history of the Sierra Nevada-Basin and Range transition zone form the last 12 Ma. In: Lageson, D.R., Peters, S.G., Lahren, M.M. (Eds.), Great Basin and Sierra Nevada, vol. 2. Geological Society of America Field Guide, pp. 97–116.
Ullah, I., and Luiz Prado, R., 2016, The analysis of HVSR curve from different ellipticity retrieval technique for a single 3c-station recording: *Nat. Haz. Earth Syst. Sci. Discuss.*, 19 pp., doi: 10.5194/nhess-2016-370.
U.S. Bureau of Labor Statistics, 2022, All Reno, NV area manufacturing employment history: Last accessed 20 May 2022, https://data.bls.gov/
U.S. Census Bur., 2021, 2020 Census redistricting data: Accessed 20 May 2022, data.census.gov/cedsci/
Widmer, M., 2023, A collection of data from 17 studies in Washoe County shared for use in this study: HYDRO-GEO Consulting Services, Ltd. P.O. Box 1022, Verdi, NV 89439
Wesnousky, S.G., 2005a. Active faulting in the walker Lane. Tectonics 24, TC3009 https://doi.org/10.1029/2004TC001645.
Wesnousky, S.G., 2005b. The San Andreas and Walker Lane fault systems, western North America: transpression, transtension, cumulative slip and the structural evolution of a major transform plate boundary. J. Struct. Geol. 27, 1505–1512.
WorldAtlas.com, 2022, World's largest industrial areas: Last accessed 22 May 2022, https://www.worldatlas.com/articles/world-s-largest-industrial-areas.html